



Synthesis, Crystal Structure, and Luminescence Properties of the Iso-Reticular Series of Lanthanide Coordination Polymers Synthesized from Hexa-Lanthanide Molecular Precursors

Haiyun Yao, Guillaume Calvez, Carole Daiguebonne, Yan Suffren, Kevin Bernot, Thierry Roisnel, Olivier Guillou

► To cite this version:

Haiyun Yao, Guillaume Calvez, Carole Daiguebonne, Yan Suffren, Kevin Bernot, et al.. Synthesis, Crystal Structure, and Luminescence Properties of the Iso-Reticular Series of Lanthanide Coordination Polymers Synthesized from Hexa-Lanthanide Molecular Precursors. *Inorganic Chemistry*, 2022, 61 (12), pp.4895-4908. 10.1021/acs.inorgchem.1c03654 . hal-03632067

HAL Id: hal-03632067

<https://hal.science/hal-03632067>

Submitted on 26 Apr 2022

HAL is a multi-disciplinary open access archive for the deposit and dissemination of scientific research documents, whether they are published or not. The documents may come from teaching and research institutions in France or abroad, or from public or private research centers.

L'archive ouverte pluridisciplinaire **HAL**, est destinée au dépôt et à la diffusion de documents scientifiques de niveau recherche, publiés ou non, émanant des établissements d'enseignement et de recherche français ou étrangers, des laboratoires publics ou privés.

Synthesis, crystal structure and luminescent properties of iso-reticular series of lanthanide coordination polymers synthesized from hexa-lanthanide molecular precursors

Haiyun Yao^{a, b}, Guillaume Calvez^{a, *}, Carole Daiguebonne^{a, *}, Yan Suffren^a, Kevin Bernot^{a, c}, Thierry Roisnel^a and Olivier Guillou^a.

^a Univ Rennes, INSA Rennes, CNRS UMR 6226 "Institut des Sciences Chimiques de Rennes", 35708 Rennes, France.

^b Present address: School of Opto-electronic Engineering, Zaozhuang University, Zaozhuang, 277160, China.

^c Institut Universitaire de France, 1 rue Descartes, 75005 Paris, France

* To whom correspondence should be addressed.

Carole.daiguebonne@insa-rennes.fr – guillaume.calvez@insa-rennes.fr

ABSTRACT.

Microwave-assisted reactions in DMSO, between a hexa-lanthanide octahedral complex $[\text{Ln}_6(\mu_6\text{-O})(\mu_3\text{-OH})_8(\text{NO}_3)_6(\text{H}_2\text{O})_{12}\cdot 2\text{NO}_3\cdot 2\text{H}_2\text{O}]$ with $\text{Ln} = \text{Nd-Yb}$ plus Y and either a 3-halogeno-benzoic acid (hereafter symbolized by 3-xbH with $x = \text{f}$ or c for fluoro or chloro, respectively) or a 4-halogeno-benzoic acid (hereafter symbolized by 4-xbH with $x = \text{f}$, c or b for fluoro, chloro or bromo, respectively), lead to 1D lanthanide coordination polymers. These coordination polymers are almost iso-reticular. The crystal structure is described on the basis of the coordination polymer with chemical formula $[\text{Tb}(\text{4-fb})_3(\text{DMSO})(\text{H}_2\text{O})_2\cdot \text{DMSO}]_\infty$ obtained from 4-fluorobenzoic acid (4-fbH) and the Tb^{3+} -based octahedral complex: It crystallizes in the triclinic system, space group $P\bar{1}$ ($n^\circ 2$), with the following cell parameters: $a = 9.8561(9) \text{ \AA}$, $b = 10.5636(9) \text{ \AA}$, $c = 15.1288(15) \text{ \AA}$, $\alpha = 100.840(3)^\circ$, $\beta = 95.552(3)^\circ$, $\gamma = 110.482(3)^\circ$, $V = 1426.4(3) \text{ \AA}^3$ and $Z = 2$. It can be described on the basis of 1D molecular chains. Luminescence properties of the Tb- and Eu-derivatives have been measured and compared *versus* the halogeno-function and its position (*meta* or *para*). Some molecular alloys have also been prepared in order to estimate the strength of the intermetallic energy transfers. In order to confirm that the hexa-nuclear complexes (and not the halogenated ligand) have a structuring effect for the formation of the straight chain-like molecular motif, another coordination polymer with chemical formula $[\text{Tb}(\text{4-npa})_3\text{DMSO}\cdot \text{DMSO}\cdot \text{H}_2\text{O}]_\infty$ where 4-npaH symbolizes 4-nitro-phenyl-acetic acid, has been prepared. It crystallizes in the triclinic system, space group $P\bar{1}$ ($n^\circ 2$) with the following cell parameters: $a = 7.8784(8) \text{ \AA}$, $b = 14.8719(16) \text{ \AA}$, $c = 15.2753(17) \text{ \AA}$, $\alpha = 73.612(4)^\circ$, $\beta = 86.406(4)^\circ$, $\gamma = 83.104(4)^\circ$, $V = 1703.8(3) \text{ \AA}^3$ and $Z = 2$. Its crystal structure can be described on the basis of a molecular motif that is similar to the one observed in the five previous crystal structures which confirms the structuring effect of the hexa-nuclear complexes.

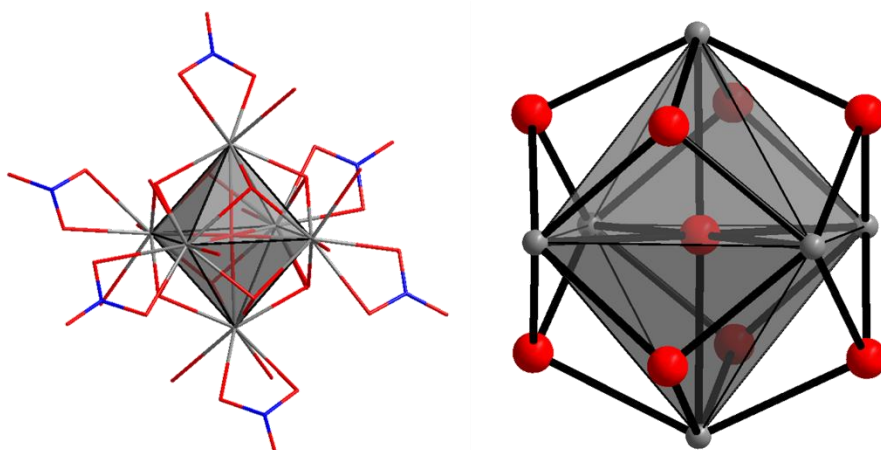
INTRODUCTION.

Lanthanide-based coordination compounds, complexes or coordination polymers,¹ have been widely studied in the last two decades. Indeed, because of the unique physical and chemical properties of the lanthanide ions,²⁻³ these compounds exhibit interesting magnetic⁴⁻⁶ and optical properties⁷⁻⁸ that make them promising candidates in various technological fields such as molecular thermometry,⁹⁻¹⁰ chemical sensing,¹¹⁻¹⁴ light and display¹⁵⁻¹⁶ or fight against counterfeiting,¹⁷⁻²⁰ for instance. All these potential applications require highly emissive materials and therefore the quest for new lanthanide-based coordination compounds exhibiting bright luminescence constitutes a continuous concern.²¹⁻²⁸

The strategy that consists on focusing on the choice of the ligand is, by far, the most commonly followed.^{15-16, 29-30} The works along this line have demonstrated that the ligands must present a structuring effect (via π -stacking interactions, hydrogen- or halogen-bonds), an efficient antenna effect³¹ and a good chemical affinity toward lanthanide ions. Halogeno-derivatives of benzene-poly-carboxylic acids fill these requirements: (i) their extended π -system allows a good efficiency as sensitizer and provides structuring π -stacking interactions; (ii) their carboxylate functions have excellent chemical affinity for the lanthanide ions that are hard Pearson's acids;³²⁻³³ (iii) halogens can induce halogen-bonds³⁴ that keep away from each other the molecular motifs which is beneficial for reducing concentration quenching³⁵ and contribute to insure the crystal packing robustness. Consequently, numerous lanthanide-based coordination polymers involving this family of ligands and exhibiting interesting luminescent properties have been described so far.^{17, 36-37}

An alternative strategy consists on using no longer isolated single lanthanide ions but polymetallic complexes as reactants. Actually, numerous coordination polymers with poly-lanthanide metallic sites have been described so far.³⁸⁻⁴³ However, most of the

poly-lanthanide complexes have been obtained from serendipitous one-pot synthesis and are not stable enough for being used as molecular precursors.⁴⁴ To date, the only poly-lanthanide oxo-hydroxo complexes that have been used as starting reactants are the octahedral hexa-nuclear complexes first described by Giester *et al.*⁴⁵⁻⁴⁹ These complexes have general chemical formula $[\text{Ln}_6(\mu_6\text{-O})(\mu_3\text{-OH})_8(\text{H}_2\text{O})_{12}(\text{NO}_3)_6 \cdot 2\text{NO}_3 \cdot 2\text{H}_2\text{O}]$ hereafter abbreviated as $[\text{Ln}_6]$.⁵⁰ The structure of the octahedral core can be described based on an octahedron with a lanthanide ion at each vertex, a central $\mu_6\text{-O}^{2-}$ ion and eight $\mu_3\text{-OH}^-$ anions that cap the eight triangular faces (Scheme 1). Additionally, a bidentate nitrate ion binds each lanthanide ion whose surrounding is completed by two coordination water molecules.



Scheme 1. Projection views of $[\text{Y}_6(\mu_6\text{-O})(\mu_3\text{-OH})_8(\text{H}_2\text{O})_{12}(\text{NO}_3)_6]^{2+}$ and of the hexa-nuclear core $[\text{Y}_6(\mu_6\text{-O})(\mu_3\text{-OH})_8]^{8+}$. The central $\mu_6\text{-O}^{2-}$ ion polyhedron is drawn. Redrawn from reference 50.

Hexa-lanthanide complexes are prepared by hydrolysis of lanthanide nitrates by careful addition of a sodium hydroxide solution.⁵⁰ This synthetic pathway requires a subtle control of the different experimental parameters (pH, concentrations, temperature...) because the complexes are obtained in a narrow pH range (Figure S1).⁵⁰ Indeed, if the solution is too acidic, hydrated lanthanides ions remain isolated and if it is too basic, very stable insoluble polymeric species such as $\text{Ln}(\text{NO}_3)(\text{OH})_2 \cdot \text{H}_2\text{O}$,⁵¹⁻⁵² $\text{LnO}(\text{NO}_3)$ ⁵³ or $\text{Ln}(\text{OH})_3$ ⁵⁴ are produced. Therefore, these complexes must be used as molecular precursors with ligands that do not make the pH of the reacting medium too high nor too low. Otherwise their octahedral

structure is destroyed.⁵⁰ Additionally it has been shown that these complexes are soluble in polar solvent but collapse rapidly. On the opposite, they are stable but only very slightly soluble in non-polar solvent.⁵⁰ Acetonitrile is a good compromise and a coordination polymer with octahedral complexes as metallic centers and terephthalate as ligand (Figure 1) has been obtained previously in this solvent.⁵⁵

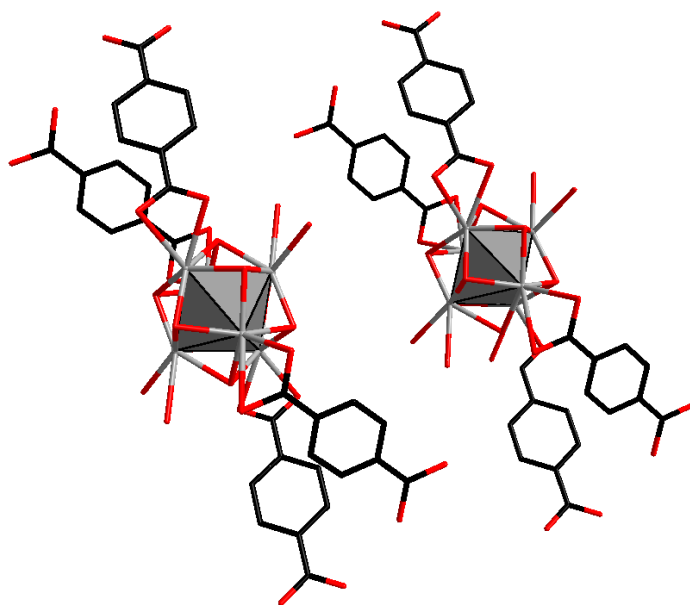
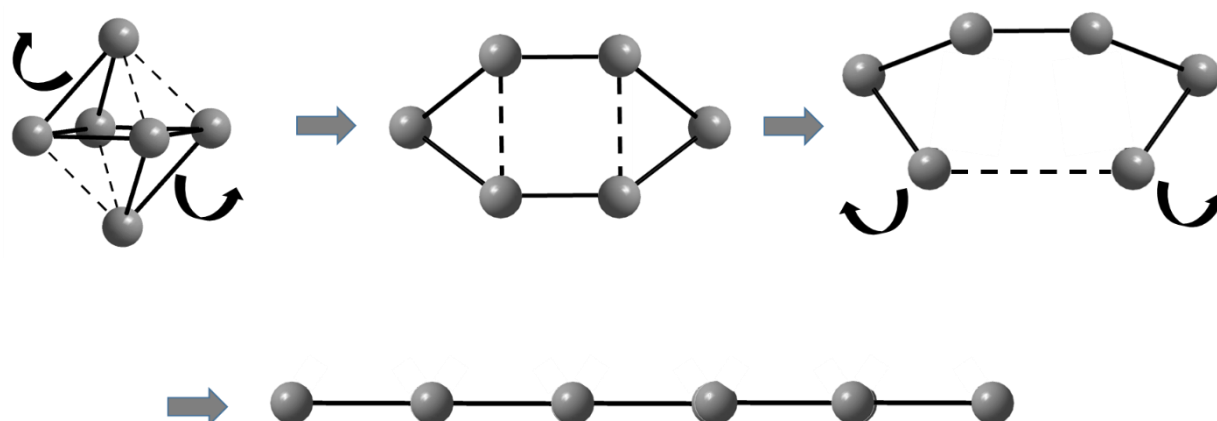


Figure 1. Schematic representation of two neighboring chain-like molecular motifs in $\{[Ln_6O(OH)_8](NO_3)_2(bdc)(Hbdc)_2 \cdot 2NO_3 \cdot H_2bdc\}_\infty$ where H_2bdc symbolizes terephthalic acid (CCDC-784583). Redrawn from reference 56.

However, it has been shown that even when the octahedral complexes collapse, their use as molecular precursors leads to lanthanide-based coordination polymers that cannot be obtained from usual lanthanide salts such as chloride or nitrate salts.⁵⁷⁻⁶⁰ For instance it has recently been shown that microwave-assisted reaction in acetonitrile of an octahedral hexa-nuclear complex with a 3-halogenobenzoic acid leads to complexes in which the hexa-lanthanide core is no longer an octahedron but a planar hexagon.⁵⁹⁻⁶⁰ A reactional mechanism was proposed, for explaining the octahedron \rightarrow hexagon transformation that assumed that the carboxylate ligand clips neighboring lanthanide ions, which provokes the separation and the gliding of two opposite triangular faces of the octahedron (Scheme 2). More recently, it has been shown that microwave-assisted reaction in acetonitrile, between the

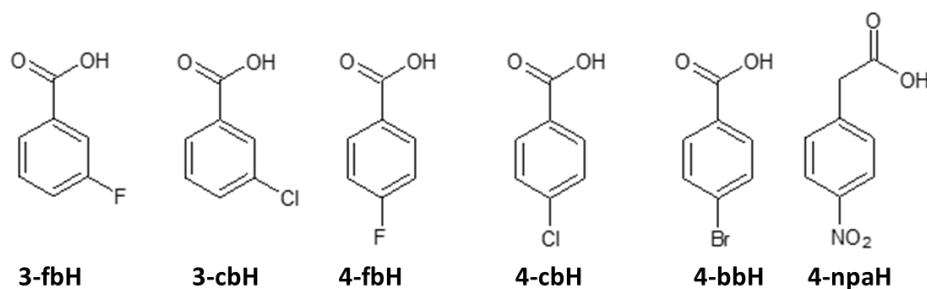
same hexa-lanthanide molecular precursor and 2-bromobenzoic acid as ligands, followed by a maturation period in a closed vessel leads to straight molecular chains (Scheme 2).⁶¹ It was assumed that during the maturation the hydrolysis goes on and provokes the opening out of the hexagons. Luminescence evidences support this assumption but the driving force (halogen-bonds, hydrolysis, carboxylate clip...) of these structural transformations is still unclear.



Scheme 2. Suggested mechanism octahedron \rightarrow hexagon \rightarrow chain that has been previously suggested for similar systems. Broken lines represent the bonds that are broken. Drawn from reference 61.

In this paper, in order to investigate this point, five new series of lanthanide-based coordination polymers are synthesized by microwave-assisted reaction in DMSO (a solvent that favors hydrolysis of the molecular precursors)⁵⁰ between octahedral hexa-nuclear complexes and 3-halogenobenzoic or 4-halogeno-benzoic acids. These compounds are structurally described and their luminescent properties studied.

All the compounds that belong to these five families are pseudo-iso-reticular. In order to show that not the halogenated ligands but the hexa-nuclear molecular precursor is responsible for the formation of straight chain-like molecular motifs, a coordination polymer has been prepared from the Tb-based hexa-nuclear complex and 4-nitro-phenyl-acetate (Scheme 3) as ligand, in identical experimental conditions. Its crystal structure is described and compared to that obtained with the halogeno-benzoate ligands.



Scheme 3. Ligands that have been used in this work. From left to right: 3-fluoro-benzoic acid (3-fbH), 3-chloro-benzoic acid (3-cbH), 4-fluoro-benzoic acid (4-fbH), 4-chloro-benzoic acid (4-cbH), 4-bromo-benzoic acid (4-bbH) and 4-nitro-phenyl-acetic acid (4-npaH).

EXPERIMENTAL SECTION.

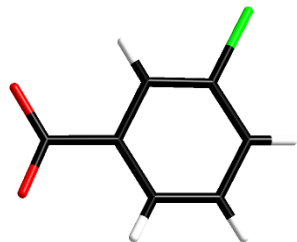
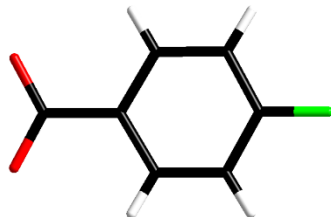
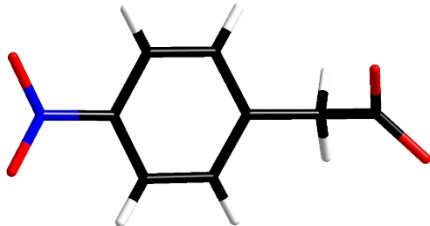
Lanthanide oxides (4N) were purchased from Ampère Company and used without further purification. Hydrated lanthanide nitrates were prepared according to established procedures.⁶² Homo- and hetero-lanthanide octahedral molecular precursors were prepared as previously described.^{56, 63} 3-halogenobenzoic, 4-halogenobenzoic and 4-nitro-phenyl-acetic acids (> 98 %) were purchased from TCI and used without further purification.

Synthesis of the coordination polymers.

0.05 mmol of a hexa-nuclear complex ($[Ln_6]$) and 0.05 mmol of one of the halogeno-benzoic acids or of 4-nitro-phenyl-acetic acid were mixed under stirring at room temperature with 1 mL of DMSO. The suspension was microwave-heated at 100°C for 20 min (150 W of power setting and 2 bars of maximum pressure in a CEM Discover microwave heater). Then the resulting clear solution was allowed to cool to room temperature and left in a closed vessel for a few days. Single crystals appeared that were filtered, washed with DMSO and dried in air. Each batch produced only about 200 μ g of single crystals which make some measurements tricky. Isostructurality of the compounds that constitute a series was assumed on the basis of their powder X-ray diffraction diagrams as well as of their IR spectra. They were recorded on the basis of sample made of crushed single crystals. Simulated powder X-ray diffraction diagrams that we used as references are reported in

Figure S2. Compounds that have been prepared according to this procedure are listed in Table 1. Iso-structural hetero-lanthanide molecular alloys have been prepared from the corresponding hetero-lanthanide octahedral complexes according to the same procedure. Relative metallic contents have been estimated by EDS measurements (Tables S1 to S3).

Table 1. Synthesized coordination polymers.

Chemical formula Abbreviation	Ln^{3+}	Ligand
$[\text{Ln}(\text{3-fb})_3(\text{DMSO})(\text{H}_2\text{O})_2 \cdot \text{DMSO}]_\infty$ Abbreviated by $[\text{Ln}(\text{3-fb})]_\infty$	Sm^{3+} , Eu^{3+} , Gd^{3+} , Tb^{3+} , Dy^{3+} , Y^{3+}	 3-fb = 3-fluorobenzoate 3-cb = 3-chlorobenzoate
$[\text{Ln}(\text{3-cb})_3(\text{DMSO})(\text{H}_2\text{O})_2 \cdot \text{DMSO}]_\infty$ Abbreviated by $[\text{Ln}(\text{3-cb})]_\infty$	Sm^{3+} , Eu^{3+} , Gd^{3+} , Tb^{3+} , Dy^{3+} , Y^{3+}	
$[\text{Ln}(\text{4-fb})_3(\text{DMSO})(\text{H}_2\text{O})_2 \cdot \text{DMSO}]_\infty$ Abbreviated by $[\text{Ln}(\text{4-fb})]_\infty$	Nd^{3+} , Eu^{3+} , Tb^{3+} , Dy^{3+}	 4-fb = 4-fluorobenzoate 4-cb = 4-chlorobenzoate 4-bb = 4-bromobenzoate
$[\text{Ln}(\text{4-cb})_3(\text{DMSO})(\text{H}_2\text{O})_2 \cdot \text{DMSO}]_\infty$ Abbreviated by $[\text{Ln}(\text{4-cb})]_\infty$	Nd^{3+} , Sm^{3+} , Eu^{3+} , Gd^{3+} , Tb^{3+} , Dy^{3+} , Ho^{3+} , Er^{3+} , Tm^{3+} , Yb^{3+}	
$[\text{Ln}(\text{4-bb})_3(\text{DMSO})(\text{H}_2\text{O})_2 \cdot \text{DMSO}]_\infty$ Abbreviated by $[\text{Ln}(\text{4-bb})]_\infty$	Sm^{3+} , Eu^{3+} , Tb^{3+} , Dy^{3+} , Ho^{3+} , Er^{3+}	
$[\text{Ln}(\text{4-npa})_3\text{DMSO} \cdot \text{DMSO} \cdot \text{H}_2\text{O}]_\infty$ Abbreviated by $[\text{Ln}(\text{4-npa})]_\infty$	Tb^{3+}	 4-npa = 4-nitro-phenyl-acetate

Ln^{3+} in bold indicates the Ln^{3+} -derivative on the basis of which crystal structure has been solved.

X-ray diffraction.

Powder X-ray diffraction diagrams were collected with a Panalytical X'Pert Pro diffractometer equipped with an X'Celerator detector. Typical recording conditions were: 45 kV, 40 mA, Cu K_α radiation ($\lambda = 1.542 \text{ \AA}$), θ/θ mode. Simulated patterns from crystal structure were produced with PowderCell and WinPLOTR programs.⁶⁴⁻⁶⁵

Single crystals were mounted on a Bruker D8 Venture diffractometer (except [Y(3-fb)]_∞ that has been mounted on a Bruker APEXII). Crystal data collection were performed at 150 K with Mo K_α radiation ($\lambda = 0.70713 \text{ \AA}$). The crystal structures were solved and refined, using SHELX-2017⁶⁶⁻⁶⁷ with the aid of WINGX program.⁶⁸⁻⁶⁹ All non-hydrogen atoms were refined anisotropically. Hydrogen atoms were located at ideal positions. Absorption corrections were performed using the facilities of WINGX program.⁷⁰ Selected crystal and final structure refinement data are gathered in Table 2. Full details of the crystal structures have been deposited with the Cambridge Crystallographic Data Centers under the depositary numbers CCDC-1871210, CCDC-1871227, CCDC-1871217, CCDC-1871208, CCDC-1871228 and CCDC-1871216 for [Y(3-fb)₃(DMSO)(H₂O)₂·DMSO]_∞, [Tb(3-cb)₃(DMSO)(H₂O)₂·DMSO]_∞, [Tb(4-fb)₃(DMSO)(H₂O)₂·DMSO]_∞, [Tb(4-cb)₃(DMSO)(H₂O)₂·DMSO]_∞, [Sm(4-bb)₃(DMSO)(H₂O)₂·DMSO]_∞ and [Tb(4-npa)₃DMSO·DMSO·H₂O]_∞, respectively.

Table 2. Crystal and final refinement data for [Y(3-fb)] _∞ , [Tb(3-cb)] _∞ , [Tb(4-fb)] _∞ , [Tb(4-cb)] _∞ , [Sm(4-bb)] _∞ and [Tb(4-npa)] _∞						
	[Y(3-fb)] _∞	[Tb(3-cb)] _∞	[Tb(4-fb)] _∞	[Tb(4-cb)] _∞	[Sm(4-bb)] _∞	[Tb(4-npa)] _∞
Chemical formula	C ₂₅ H ₂₇ F ₃ O ₁₀ S ₂ Y	C ₂₅ H ₂₈ Cl ₃ O ₁₀ S ₂ Tb	C ₂₅ H ₂₈ F ₃ O ₁₀ S ₂ Tb	C ₂₅ H ₂₈ Cl ₃ O ₁₀ S ₂ Tb	C ₂₅ H ₂₈ Br ₃ O ₁₀ S ₂ Sm	C ₂₈ H ₃₂ N ₃ O ₁₅ S ₂ Tb
System	Triclinic	Triclinic	Triclinic	Triclinic	Triclinic	Triclinic
Space group (n°)	<i>P</i> $\bar{1}$ (n°2)	<i>P</i> $\bar{1}$ (n°2)	<i>P</i> $\bar{1}$ (n°2)	<i>P</i> $\bar{1}$ (n°2)	<i>P</i> $\bar{1}$ (n°2)	<i>P</i> $\bar{1}$ (n°2)
Formula weight (g.mol ⁻¹)	697.49	817.86	768.51	817.86	942.67	873.62
<i>a</i> (Å)	9.9216(10)	9.9210(9)	9.8561(9)	9.9200(11)	9.8646(11)	7.8784(8)
<i>b</i> (Å)	10.5489(9)	10.4686(9)	10.5636(9)	10.8153(11)	10.7609(11)	14.8719(16)
<i>c</i> (Å)	14.8600(16)	16.8789(16)	15.1288(15)	15.9764(16)	16.2446(18)	15.2753(17)
α (°)	100.764(3)	101.503(3)	100.840(3)	100.855(4)	100.103(4)	73.612(4)
β (°)	94.826(4)	101.950(3)	95.552(3)	96.974(4)	98.015(4)	86.406(4)
γ (°)	109.091(3)	108.209(3)	110.482(3)	108.401(4)	108.204(4)	83.104(4)
<i>V</i> (Å ³)	1426.1(2)	1562.0(3)	1426.4(2)	1567.0(3)	1577.5(3)	1703.8(3)
<i>Z</i>	2	2	2	2	2	2
<i>D</i> _{calc} (g.cm ⁻³)	1.624	1.739	1.789	1.733	1.985	1.699
<i>R</i> (%)	3.11	1.85	4.04	3.83	4.16	2.87
<i>R</i> _w (%)	7.92	4.41	10.66	10.55	9.87	7.27
<i>GoF</i>	1.04	1.199	1.195	1.179	1.055	1.204
CCDC number	1871210	1871227	1871217	1871208	1871228	1871216

Electronic microscopy and Energy Dispersive Spectroscopy (EDS).

EDS measurements have been performed with a Hitachi TM-1000, Tabletop Microscope version 02.11 (Hitachi High-Technologies, Corporation Tokyo Japan) with EDS analysis system (SwiftED-TM, Oxford Instruments Link INCA). Reproducibility of the elemental analyses has been checked by repeating the measurements several times. Results, expressed in atom percentages, are average values of different spots. These experiments support the homogeneity of the samples.

Optical measurements.

Optical measurements have been performed on single crystals. Solid-state emission and excitation spectra have been measured on a Horiba Jobin-Yvon Fluorolog III fluorescence spectrometer equipped with a Xe lamp 450 W, an UV-Vis photomultiplier (Hamamatsu R928, sensitivity 190 - 860 nm). The emission/excitation spectra recordings were realized in quartz cuvettes. The quantum yields were calculated using a F-3018 HJY integrating sphere, extending its correction curve in the 290–330 nm range by measuring europium tris(dipicolinate) in a tris(hydroxymethyl)aminomethane (Tris) buffer solution as a standard, as proposed by Chauvin *et al.*⁷¹ The quantum yields have been calculated by measuring the ratio between the absorbed photons around the excitation wavelength with and without the sample and the emitted photons with and without the sample. The lifetime values were measured using a pulsed xenon source with the same device and measuring the intensity emitted after increasing time delay. The decay times were fitted using a mono-exponential decay function. Appropriate filters were used to remove the residual excitation laser light, the Rayleigh scattered light and associated harmonics from spectra. All spectra were corrected for the instrumental response function. Colorimetric coordinates have been calculated on the basis of the emission spectra.⁷²⁻⁷³

RESULTS AND DISCUSSION

Microwave-assisted reactions of a hexa-nuclear complex with an halogeno-benzoic acid (3-fluorobenzoic acid (3-fbH), 3-chloro-benzoic acid (3-cbH), 4-fluoro-benzoic acid (4-fbH) 4-chloro-benzoic acid (4-cbH) or 4-bromo-benzoic acid (4-bbH)) lead to five series of isostructural coordination polymers with respective chemical formula $[\text{Ln}(\text{3-fb})_3(\text{DMSO})(\text{H}_2\text{O})_2 \cdot \text{DMSO}]_\infty$ with $\text{Ln} = \text{Sm-Dy}$ plus Y, $[\text{Ln}(\text{3-cb})_3(\text{DMSO})(\text{H}_2\text{O})_2 \cdot \text{DMSO}]_\infty$ with $\text{Ln} = \text{Sm-Dy}$ plus Y, $[\text{Ln}(\text{4-fb})_3(\text{DMSO})(\text{H}_2\text{O})_2 \cdot \text{DMSO}]_\infty$ with $\text{Ln} = \text{Nd, Eu, Tb, Dy}$, $[\text{Ln}(\text{4-cb})_3(\text{DMSO})(\text{H}_2\text{O})_2 \cdot \text{DMSO}]_\infty$ with $\text{Ln} = \text{Nd-Yb}$ and $[\text{Ln}(\text{4-bb})_3(\text{DMSO})(\text{H}_2\text{O})_2 \cdot \text{DMSO}]_\infty$ with $\text{Ln} = \text{Sm, Eu, Tb, Dy, Ho, Er}$. These five series are hereafter abbreviated by $[\text{Ln}(\text{3-fb})]_\infty$, $[\text{Ln}(\text{3-cb})]_\infty$, $[\text{Ln}(\text{4-fb})]_\infty$, $[\text{Ln}(\text{4-cb})]_\infty$ and $[\text{Ln}(\text{4-bb})]_\infty$, respectively. The crystal structure of the first family has been solved on the basis of the Y-derivative, that of the three following families on the basis of the Tb-derivatives and that of the last family on the basis of the Sm-derivative. Despite great efforts it has not be possible to obtain these crystalline phases from usual lanthanide salts (chloride nor nitrate) which strongly suggests a structuring effect of the hexa-nuclear complexes used as reactants.

All these five crystal structures are almost iso-reticular and therefore only the crystal structure of $[\text{Tb}(\text{4-fb})]_\infty$ is described in details in the following. Projection views of the four other families are drawn in Figures S3 to S6. Some characteristic numerical values for the five crystal structures are gathered in Tables S4-S6 for comparison.

Crystal structure of $[\text{Tb}(\text{4-fb})]_\infty$

There is only one independent Tb^{3+} ion in this crystal structure. The crystal structure can be described on the basis of a straight chain-like molecular motif that spreads along the

a-axis (the angle formed by three consecutive Tb³⁺ ions in a molecular chain is 171.090(2) °) (Figure 2 and Table S4). This structural feature supports again the hexa-nuclear complexes structuring effect. Indeed, similar straight chain-like molecular motifs have already been observed previously for coordination polymers prepared from hexa-nuclear reactants.⁶¹ The Tb³⁺ ion is eight coordinated by eight oxygen atoms that form a slightly distorted triangular dodecahedron (Continuous Shape Measurements(CShM)⁷⁴ agreement factor is 0.938) (Table S5). Two oxygen atoms are from two coordination water molecules, one from one DMSO coordination molecule and five from five different 4-fb⁻ ligands (Figure 2). There are three independent 4-fb⁻ ligands: one is unidentate and the two others are bridging (μ_2 : η_1 - η_1) (Figure 2). Tb³⁺ ions are linked to each other by two bridging ligands and the Tb...Tb distance between adjacent Tb³⁺ ions in the chain-like molecular motif is 5.0422(5) Å on one side and 4.8437(4) Å on the other side (Table S4).

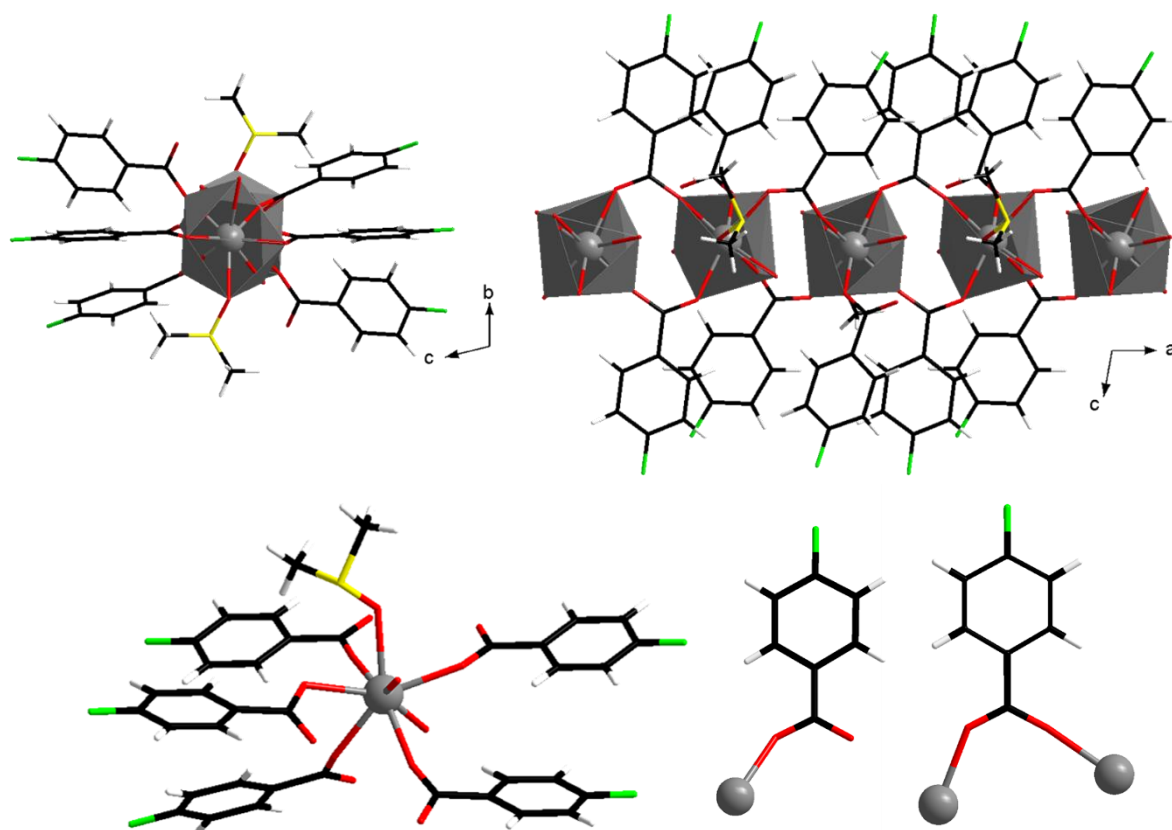


Figure 2. Top: Projection views along the *a*-axis (left) and along the *b*-axis (right) of [Tb(4-fb)]_∞. Tb polyhedrons are drawn. Bottom: neighborhood of the Tb³⁺ ion (left) and coordination modes of the 4-fb⁻ ligands (right) in [Tb(4-fb)]_∞.

which intermetallic energy transfers are expected to be less efficient⁷⁵) are lanthanide ions that belong to the same chain-like molecular motif.

These five crystal structures are very similar (Tables S4-S6) and present only slight structural differences. Unexpectedly, neither the nature of the halogen group or its position (*meta* or *para*) significantly influence the crystal structure. This support again the structuring effect of the hexa-nuclear molecular precursor.

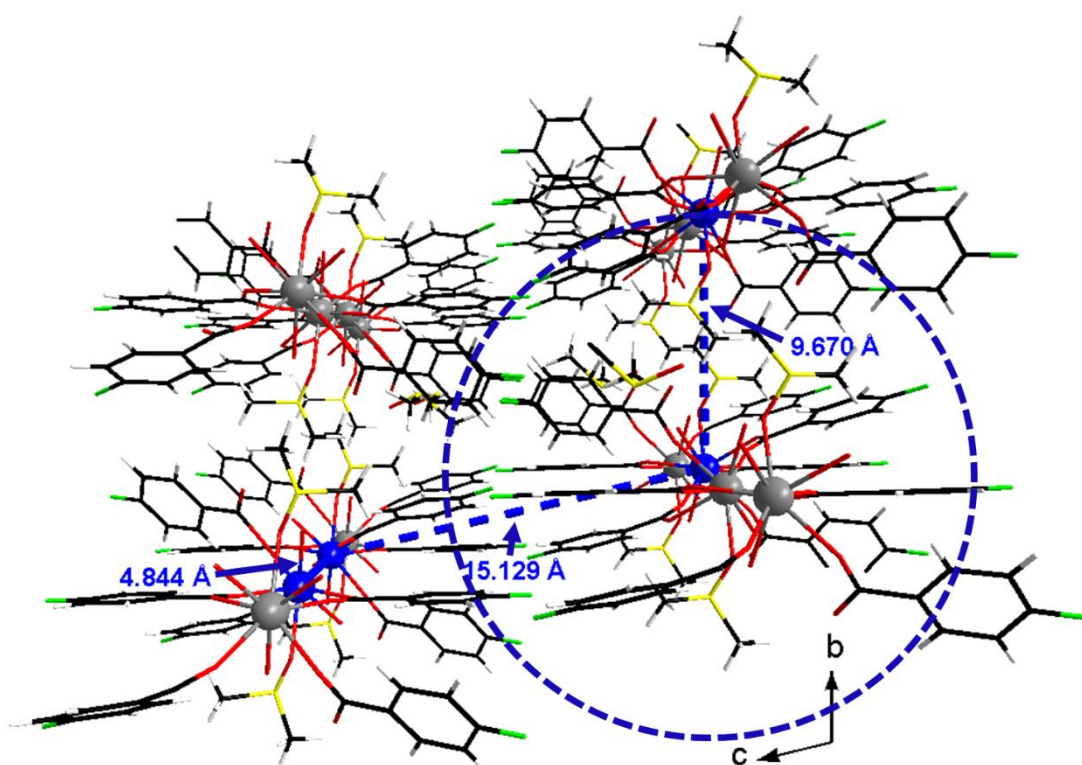


Figure 4. Perspective view, along the *a*-axis of $[\text{Tb}(4\text{-fb})]_{\infty}$. Shortest intermetallic distances along the *a*-, *b*- and *c*-axis are reported. The radius of the dotted blue circle is 10 Å.

Luminescent properties of the Tb- and Eu-derivatives.

Because of their potentially interesting luminescent properties in the visible domain, only the Tb- and Eu-derivatives are described hereafter. Their room temperature solid-state excitation and emission spectra have been recorded (Figures 5 and 6). Quantum yields and luminescent lifetimes have been measured (Table 3) and colorimetric coordinates under UV irradiation have been calculated from emission spectra⁷² (Table S7).

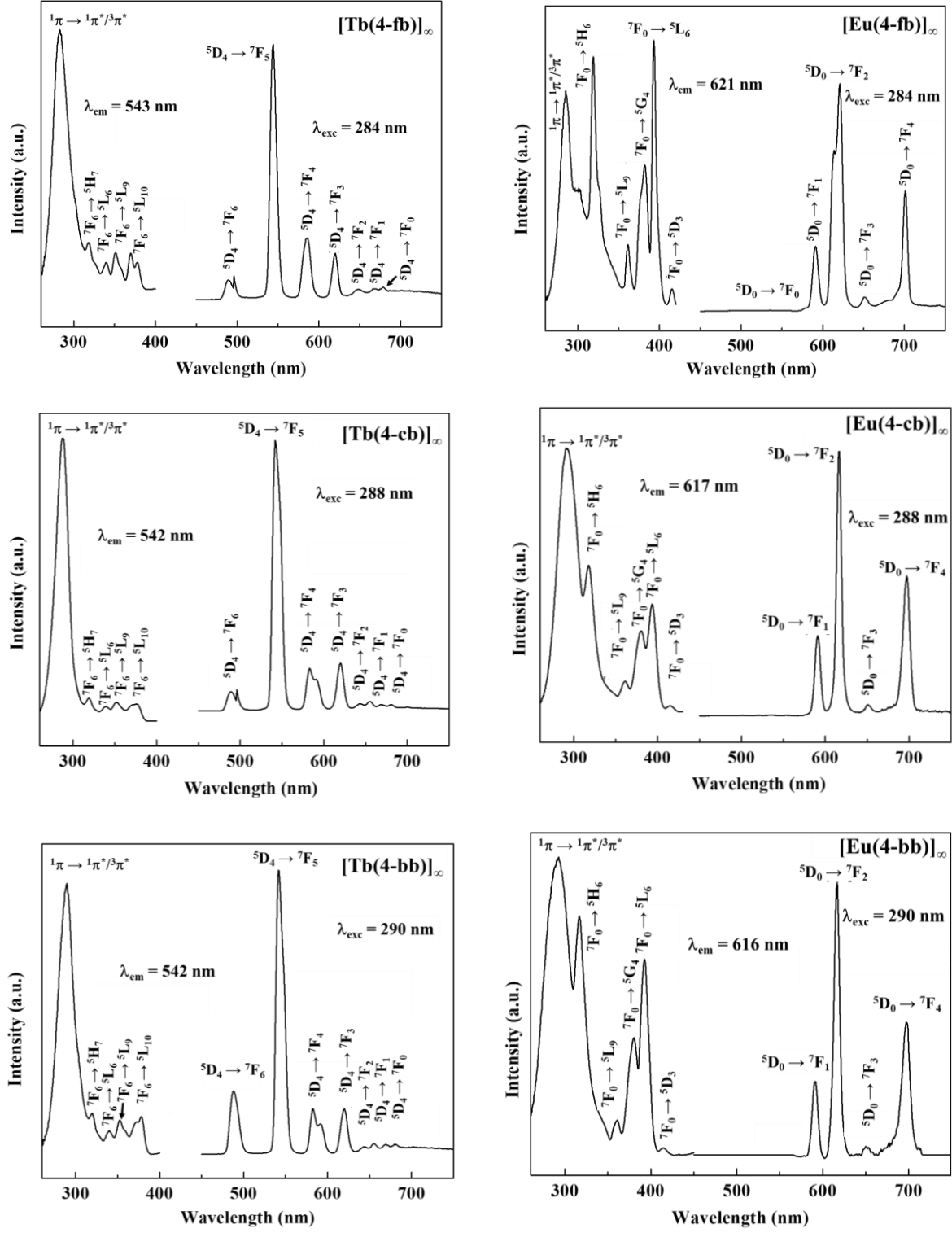


Figure 5. Room temperature solid-state excitation and emission spectra of the Tb- (left) and Eu-derivatives (right) of [Ln(4-fb)]_∞ (top), [Ln(4-cb)]_∞ (middle) and [Ln(4-bb)]_∞ (bottom).

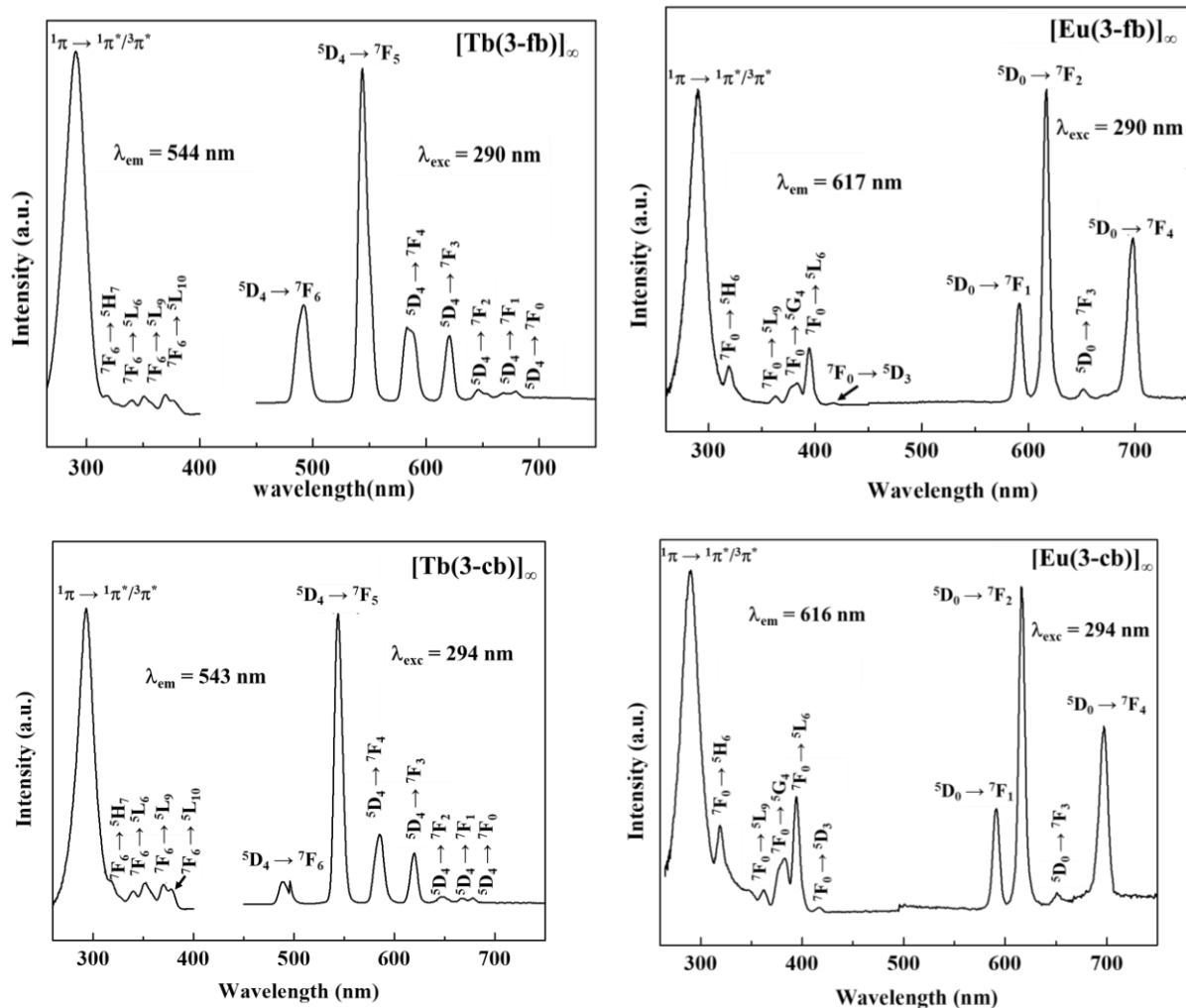


Figure 6. Room temperature solid-state excitation and emission spectra of the Tb- (left) and Eu-derivatives (right) of $[\text{Ln}(\text{3-fb})]_{\infty}$ (top), $[\text{Ln}(\text{3-cb})]_{\infty}$ (bottom).

Excitation spectra (Figures 5 and 6) indicate that all the ligands present an efficient antenna effect³¹ toward both the Eu- and the Tb-derivatives. Indeed, all excitation spectra present a sizeable maximum between 284 nm and 290 nm that can be attributed to $1\pi^*/3\pi^* \leftarrow 1\pi$ transition of the ligands. However, it can be noticed that the excitation spectra of the Eu-derivatives also present very sizeable excitation peaks that correspond to direct excitation of the Eu^{3+} ions. For instance, $5\text{L}_6 \leftarrow 7\text{F}_0$ and $5\text{H}_6 \leftarrow 7\text{F}_0$ transitions at about 395 nm and 320 nm, respectively, are particularly intense.⁷⁶⁻⁷⁷ These intense relative intensities can be related to a PET mechanism (Photoinduced Electron Transfer) that is efficient when there is a donor atom in the vicinity of an easily reducible lanthanide ions such as Eu^{3+} .^{14, 78-82}

Room Temperature solid-state emission spectra (Figures 5-6) of all the Tb-derivatives are similar. They show the characteristic emission peaks of the Tb³⁺ ion that correspond to the $^5D_4 \rightarrow ^7F_{J(J=6-0)}$ under ligand excitation ($\lambda_{exc} = 284\text{-}294\text{ nm}$).^{77, 83} Similarly, the room temperature solid-state emission spectra of the Eu-derivatives all exhibit the characteristic $^5D_0 \rightarrow ^7F_{J(J=0-4)}$ transitions of the Eu³⁺ ion under ligand excitation ($\lambda_{exc} = 284\text{-}294\text{ nm}$).⁷⁶⁻⁷⁷

Table 3. Excitation wavelength, overall quantum yields and luminescent lifetimes for [Ln(3-fb)]_∞, [Ln(3-cb)]_∞, [Ln(4-fb)]_∞, [Ln(4-cb)]_∞ and [Ln(4-bb)]_∞ with Ln = Tb and Eu.

	λ_{exc} (nm)	Eu		Tb	
		Q_{Eu}^{Ligand} (%)	τ_0 (ms)	Q_{Tb}^{Ligand} (%)	τ_0 (ms)
[Ln(4-fb)] _∞	284	41(4)	0.38(4)	27(3)	1.0(1)
[Ln(4-cb)] _∞	288	6.5(6)	0.11(1)	50(5)	1.0(1)
[Ln(4-bb)] _∞	290	4.7(5)	0.38(4)	24(2)	1.5(1)
[Ln(3-fb)] _∞	290	26(2)	0.46(5)	40(4)	1.1(1)
[Ln(3-cb)] _∞	294	22(2)	0.64(6)	51(5)	1.1(1)

Overall quantum yields (Table 3) of all the compounds are sizeable for both the Eu- and the Tb-derivatives. This is in agreement with efficient Ligand-to-Metal energy transfers⁵⁹ combined with the absence of high-energy vibrators in the neighborhood of the lanthanide ions.³⁵

The overall quantum yields of the Eu-derivatives support the presence of a PET mechanism. Indeed, they decrease from fluoro- to chloro- to bromo-benzoate ligands, which is in agreement with the decreasing of the electro-attractor character of the halogens from fluor to bromide.⁸⁴ As expected, the influence of the *para*-halogeno group is greater than that of the *meta*-halogeno group. Indeed, for the compounds based on 4-halogenobenzoate ligands, the overall quantum yield goes from 40% (for the fluoro-derivative) to 6% (for the chloro-derivative). For the compounds based on 3-halogenobenzoate ligands, it only goes from 26% to 22%.

Luminescence enhancement.

When lanthanide ions are close to each other, a concentration quenching is generally observed. This concentration quenching is provoked by intermetallic energy transfers⁸⁵⁻⁸⁶ and it is commonly admitted that these energy transfers are less efficient when lanthanide ions are further than 10 Å from each other.⁷⁵ Because, lanthanide ions present similar chemical properties² it is possible to prepare hetero-nuclear coordination polymers that behave as actual molecular alloys.⁸⁷⁻⁹⁰ Therefore, it is possible to separate emissive lanthanide ions by optically non-active ones.⁹¹⁻⁹² This induces an increase of the mean distance between emissive lanthanide ions and reduces the intermetallic energy transfers.

In this crystal structure, there are two lanthanide ions at about 5 Å from a given lanthanide ions and, consequently, efficient intermetallic energy transfers are expected. Therefore, we have prepared series of coordination polymers with general chemical formulas $[Y_xTb_{1-x}(4-fb)]_\infty$, $[Y_xTb_{1-x}(4-cb)]_\infty$, $[Y_xTb_{1-x}(4-bb)]_\infty$, $[Y_xTb_{1-x}(3-fb)]_\infty$ and $[Y_xTb_{1-x}(3-cb)]_\infty$ with $0 < x < 1$ (Tables S1 and S3), in which the optically non-active Y^{3+} ions act as spacers. These compounds have been prepared from the corresponding hetero-hexa-nuclear complexes $[Y_{6x}Tb_{6-6x}]$ with $0 < x < 1$ in order to avoid segregation of the two lanthanide ions.⁶¹ Their overall quantum yields and luminescent lifetimes have been measured (Table 4).

Table 4. Overall quantum yields and luminescent lifetimes of $[Y_xTb_{1-x}(4-fb)]_\infty$, $[Y_xTb_{1-x}(4-cb)]_\infty$, $[Y_xTb_{1-x}(4-bb)]_\infty$, $[Y_xTb_{1-x}(3-fb)]_\infty$ and $[Y_xTb_{1-x}(3-cb)]_\infty$ with $0 < x < 1$ under 284 nm, 288 nm, 290 nm, 290 nm and 294 nm excitation wavelength, respectively.

x	$[Y_xTb_{1-x}(4-fb)]_\infty$		$[Y_xTb_{1-x}(4-cb)]_\infty$		$[Y_xTb_{1-x}(4-bb)]_\infty$		$[Y_xTb_{1-x}(3-fb)]_\infty$		$[Y_xTb_{1-x}(3-cb)]_\infty$	
	Q_{Tb}^{Ligand} (%)	τ (ms)	Q_{Tb}^{Ligand} (%)	τ (ms)	Q_{Tb}^{Ligand} (%)	τ (ms)	Q_{Tb}^{Ligand} (%)	τ (ms)	Q_{Tb}^{Ligand} (%)	τ (ms)
0	27(3)	1.1(1)	50(5)	1.0(1)	24(2)	1.2(1)	40(4)	1.0(1)	51(5)	1.1(1)
0.05	54(5)	1.1(1)	92(9)	1.0(1)	26(3)	1.6(1)	44(4)	1.1(1)	54(5)	1.1(1)
0.1	55(5)	1.1(1)	99(9)	1.0(1)	27(3)	1.5(1)	52(5)	1.2(1)	36(4)	1.2(1)
0.2	83(8)	1.1(1)	45(4)	1.0(1)	38(4)	1.7(1)	25(2)	1.1(1)	32(3)	1.2(1)
0.5	39(4)	1.0(1)	41(4)	1.0(1)	49(5)	1.8(1)	23(2)	1.1(1)	29(3)	1.1(1)
0.7	33(3)	1.0(1)	41(4)	1.0(1)	33(3)	1.5(1)	18(2)	1.1(1)	22(2)	1.1(1)
0.9	18(2)	1.1(1)	19(2)	1.0(1)	-	-	14(1)	1.1(1)	14(1)	1.0(1)

As expected, Table 4 shows that for all series of compounds the luminescence intensity can be enhanced by dilution of the optically active Tb^{3+} ions by optically non-actives Y^{3+} . However, despite similar crystal structures, the maximum of the overall quantum yields vs x curves are not superimposed (Figure S7). From Figure S7 it can be noticed first that the dilution effect is maximum for the chloro- and fluoro-based ligands series and that only the curves that corresponds to the 4-bromobenzoate ligand-based coordination polymers presents a maximum for $x = 0.5$ that is the dilution that makes all the neighboring Tb^{3+} ions at about 10 Å from a given Tb^{3+} ion (a dilution by 50% induces a double mean $\text{Tb}\cdots\text{Tb}$ distance). All the other curves present a maximum at lower x values that is $0.05 \leq x \leq 0.2$. It can also be noticed that the influence of the position of the halogeno group is important: Indeed, the enhancement of the quantum yield in the series based on the 4-halogenobenzoate ligands is comprised between +207 % ($[\text{Y}_x\text{Tb}_{1-x}(\text{4-fb})]_\infty$) and +98 % ($[\text{Y}_x\text{Tb}_{1-x}(\text{4-bb})]_\infty$) while those based on the 3-halogenobenzoate ligands present only enhancements comprised between +30 % ($[\text{Y}_x\text{Tb}_{1-x}(\text{3-fb})]_\infty$) and +6 % ($[\text{Y}_x\text{Tb}_{1-x}(\text{3-cb})]_\infty$).

This strong diluting effect suggests efficient intermetallic energy transfers.

Efficiency of the intermetallic energy transfers.

Efficiency of the intermetallic energy transfers (η_{ET}) can be estimated according to the relationship:

$$\eta_{\text{ET}} = 1 - \frac{\tau_{\text{obs}}}{\tau_0} \quad (1)$$

where τ_{obs} and τ_0 are the luminescence lifetimes of the Tb^{3+} ion in the presence and absence of an acceptor lanthanide ion, respectively.³⁵ $[\text{Eu}_x\text{Tb}_{1-x}(\text{4-fb})]_\infty$, $[\text{Eu}_x\text{Tb}_{1-x}(\text{4-cb})]_\infty$, $[\text{Eu}_x\text{Tb}_{1-x}(\text{4-bb})]_\infty$, $[\text{Eu}_x\text{Tb}_{1-x}(\text{3-fb})]_\infty$ and $[\text{Eu}_x\text{Tb}_{1-x}(\text{3-cb})]_\infty$ with $0 < x < 1$ series have thus been prepared (Tables S2 and S3). Their emission spectra have been recorded (Figures S8 and S9) and their overall quantum yields and lifetimes have been measured (Table 5).

Table 5. Overall quantum yields, luminescent lifetimes, intermetallic energy transfers efficiency (η_{ET}) and relative intensities of the Eu^{3+} and Tb^{3+} components (F).

$[\text{Eu}_x\text{Tb}_{1-x}(4\text{-fb})]_\infty^1$						
Tb^{3+}			Eu^{3+}			
x	$Q_{\text{Tb}}^{\text{Ligand}}(\%)$	$\tau_{\text{obs}}(\text{ms})$	$Q_{\text{Eu}}^{\text{Ligand}}(\%)$	$\tau_{\text{obs}}(\text{ms})$	$\eta_{ET}(\%)$	F^\dagger
0.05	22(2)	0.7(1)	10(1)	1.1(1)	30(3)	2.91
0.1	30(3)	0.7(1)	13(1)	1.0(1)	35(3)	1.67
0.15	17(2)	0.6(1)	19(2)	0.85(8)	46(5)	0.89
0.3	9(1)	0.3(1)	26(3)	0.61(6)	77(7)	0.46
0.5	5.8(6)	0.15(1)	30(3)	0.56(6)	86(8)	0.17
$[\text{Eu}_x\text{Tb}_{1-x}(4\text{-cb})]_\infty^2$						
Tb^{3+}			Eu^{3+}			
x	$Q_{\text{Tb}}^{\text{Ligand}}(\%)$	$\tau_{\text{obs}}(\text{ms})$	$Q_{\text{Eu}}^{\text{Ligand}}(\%)$	$\tau_{\text{obs}}(\text{ms})$	$\eta_{ET}(\%)$	F^\dagger
0.05	33(3)	0.7(1)	7.7(7)	0.9(1)	26(2)	4.4
0.1	31(3)	0.6(1)	38(4)	0.9(1)	35(3)	3.8
0.15	10(1)	0.5(1)	21(2)	0.8(1)	54(5)	0.69
0.3	8.4(8)	0.3(1)	36(3)	0.6(1)	75(7)	0.34
0.5	0.22(2)	0.13(1)	35(3)	0.5(1)	88(8)	0.08
$[\text{Eu}_x\text{Tb}_{1-x}(4\text{-bb})]_\infty^3$						
Tb^{3+}			Eu^{3+}			
x	$Q_{\text{Tb}}^{\text{Ligand}}(\%)$	$\tau_{\text{obs}}(\text{ms})$	$Q_{\text{Eu}}^{\text{Ligand}}(\%)$	$\tau_{\text{obs}}(\text{ms})$	$\eta_{ET}(\%)$	F^\dagger
0.05	8.7(8)	0.6(1)	9.6(9)	0.9(1)	67(7)	0.51
0.1	4.6(4)	0.3(1)	16(2)	1.1(1)	79(8)	0.087
0.15	1.3(1)	0.2(1)	18(2)	1.0(0)	86(8)	0.04
0.3	0.33(3)	0.13(1)	24(2)	1.0(1)	92(9)	0.02
0.5	0.15(2)	0.06(1)	22(2)	0.9(1)	96(9)	0.008
$[\text{Eu}_x\text{Tb}_{1-x}(3\text{-fb})]_\infty^4$						
Tb^{3+}			Eu^{3+}			
x	$Q_{\text{Tb}}^{\text{Ligand}}(\%)$	$\tau_{\text{obs}}(\text{ms})$	$Q_{\text{Eu}}^{\text{Ligand}}(\%)$	$\tau_{\text{obs}}(\text{ms})$	$\eta_{ET}(\%)$	F^\dagger
0.05	28(3)	0.6(1)	24(2)	0.8(1)	46(4)	1.37
0.1	11(1)	0.4(1)	25(2)	0.7(1)	65(6)	0.84
0.15	4.3(4)	0.3(1)	15(1)	0.6(1)	73(7)	0.4
0.3	2.8(2)	0.3(1)	21(2)	0.7(1)	74(7)	0.176
0.5	2.1(2)	0.3(1)	42(4)	0.5(1)	70(7)	0.024
$[\text{Eu}_x\text{Tb}_{1-x}(3\text{-cb})]_\infty^5$						
Tb^{3+}			Eu^{3+}			
x	$Q_{\text{Tb}}^{\text{Ligand}}(\%)$	$\tau_{\text{obs}}(\text{ms})$	$Q_{\text{Eu}}^{\text{Ligand}}(\%)$	$\tau_{\text{obs}}(\text{ms})$	$\eta_{ET}(\%)$	F^\dagger
0.05	11(1)	0.5(1)	4.6(4)	0.5(1)	55(5)	4.2
0.1	17(1)	0.4(1)	24(2)	0.6(1)	64(6)	1.04
0.15	5.6(5)	0.3(1)	26(2)	0.6(1)	71(7)	0.38
0.3	3.2(3)	0.2(1)	29(3)	0.5(1)	85(8)	0.12
0.5	0.23(2)	0.1(1)	17(1)	0.5(1)	87(8)	0.04

¹ $\lambda_{\text{exc}} = 284 \text{ nm}$; ² $\lambda_{\text{exc}} = 288 \text{ nm}$; ³ $\lambda_{\text{exc}} = 290 \text{ nm}$; ⁴ $\lambda_{\text{exc}} = 290 \text{ nm}$; ⁵ $\lambda_{\text{exc}} = 294 \text{ nm}$

[†] F is equal to the ratio of the maximum intensity of the major Tb^{3+} emission peak ($\text{Tb}: {}^5\text{D}_4 \rightarrow {}^7\text{F}_5$) over the maximum intensity of the major Eu^{3+} emission peak ($\text{Eu}: {}^5\text{D}_0 \rightarrow {}^7\text{F}_2$)

At first glance, results gathered in Table 5 show that intermetallic energy transfers are important for all the compounds of the five families. However, a more detailed analysis indicates that intermetallic energy transfers are more important for compounds that are based on the heaviest halogen-derivatives. For instance, the compounds with general chemical formula $[\text{Eu}_x\text{Tb}_{1-x}(\text{4-bb})]_\infty$ exhibit very high intermetallic energy transfers efficiencies ranging from 67% (for $x = 0.05$) to 96% (for $x = 0.5$). In agreement with what is observed for the Y^{3+} -containing derivatives, the compounds based on the ligands with a *meta*-halogeno group present higher intermetallic energy transfers efficiencies for low x values than the compounds based on the ligands with a *para*-halogeno group. On another hand, their intermetallic energy transfers efficiencies increase slower *versus* x .

Intermetallic energy transfers have been widely studied for many years.⁹³⁻⁹⁴ It has been shown that two mechanism can be at their origin: (i) The first one is due to electrostatic interactions and is independent of the concentrations of both the donor and the acceptor. It relies only on a well defined donor/acceptor pair and is encountered in molecular species.^{85, 95} (ii) The second one is encountered in doped infinite ionic materials. It is related to exchange interactions and depends on the statistical distribution of the donors and the acceptors.^{86, 96} Previous studies suggest that in lanthanide-based coordination polymers both mechanism must be taken into account.²⁴ In the present case, the above data strongly suggest that the exchange mechanism is important in these compounds. Indeed, energy transfers efficiency strongly vary *versus* the doping rate (x) and, despite similar intermetallic distances (for a given doping rate), intermetallic energy transfers efficiency vary a lot from a compounds to another. This is in agreement with exchange pathways that would vary *versus* the crystal structure. This hypothesis deserves to be studied in the future.

Table 5 also shows that, because of efficient intermetallic energy transfers, the relative intensities of the Tb^{3+} and Eu^{3+} ions contributions to the overall emission vary a lot *versus* x (See F values in Table 5). Consequently, a modulation of the luminescence color is possible by varying the relative ratio between Tb^{3+} and Eu^{3+} ions (See Figure 7 for an example. Other CIE diagrams are reported in Figure S10). Colorimetric coordinates have been calculated on the basis of the emission spectra. They are gathered in Table S8).

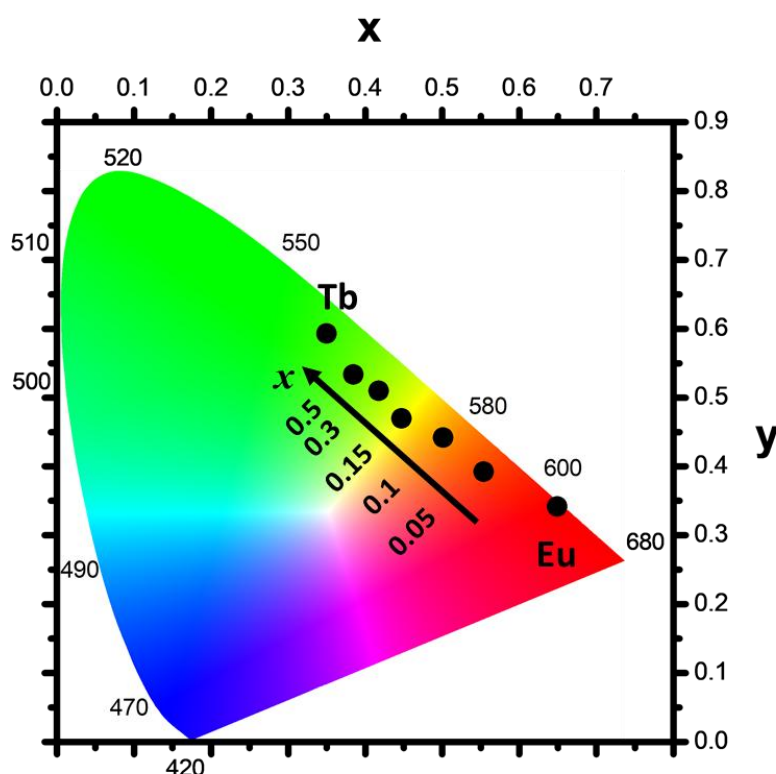


Figure 7. Colorimetric coordinates of $[\text{Eu}_x\text{Tb}_{1-x}(4\text{-fb})]_\infty$ with $0 \leq x \leq 1$ under UV irradiation ($\lambda_{\text{exc}} = 284 \text{ nm}$).

Crystal structure of $[\text{Tb}(4\text{-npa})]_\infty$.

In all the compounds described above, the crystal packing is, at least partially, insured by halogen-bonds that could be thought as being responsible of the formation of straight chain-like molecular motifs. In order to elucidate this point a compound, with chemical formula $[\text{Tb}(4\text{-npa})_3\text{DMSO} \cdot \text{DMSO} \cdot \text{H}_2\text{O}]_\infty$ has been prepared similarly to the other compounds, just replacing the halogeno-benzoic acid by 4-nitro-phenyl acetic acid. This acid was chosen because its pK_A in water ($\text{pK}_\text{A} = 3.7$)⁹⁷ is similar to those of the halogeno-benzoic

acids whose pK_A are in the range 2.8-4.1.⁹⁸ This compound has been synthesized only for the purpose of structural comparison and not for its luminescent properties. Indeed, the sp^3 carbon atom of the acetate group breaks the conjugation on the organic ligand and no efficient Tb(III) sensitization can be observed. It crystallizes in the triclinic system, space group $P\bar{1}$ ($n^\circ 2$) with the following cell parameters: $a = 7.8784(8) \text{ \AA}$, $b = 14.8719(16) \text{ \AA}$, $c = 15.2753(17) \text{ \AA}$, $\alpha = 73.612(4)^\circ$, $\beta = 86.406(4)^\circ$, $\gamma = 83.104(4)^\circ$, $V = 1703.8(3) \text{ \AA}^3$ and $Z = 2$. In the asymmetric unit, there is only one independent Tb^{3+} ion that is nine coordinated by nine oxygen atoms that form a slightly distorted spherical capped square antiprism (CShM^{74, 99} agreement factor is 1.875. See Table S9). Eight out of the nine oxygen atoms are from six different npa^- ligands and the ninth one from a coordination DMSO molecule (Figure 8). There are three crystallographically independent npa^- ligands per asymmetric unit. One is $\mu_2:\eta^1-\eta^1$ and the two others are $\mu_2:\eta^1-\eta^2$ (Figure 8). Therefore, all the ligands bind Tb^{3+} ions. This leads to straight chain-like molecular motifs (the angle formed by three adjacent Tb^{3+} ions is $167.184(6)^\circ$) decorated by npa^- ligands and coordination DMSO molecules (Figure 8). Consequently, the inorganic sub-lattice is 1D (Tb^{3+} coordination polyhedrons share edges). Intermetallic distances between neighboring Tb^{3+} ions is $3.9056(5) \text{ \AA}$ on one side and $4.0223(5) \text{ \AA}$ on the other side. Despite the change of the ligand, these structural features are very similar to that of the other crystal structures described above which strongly supports the structuring effect of the octahedral hexa-nuclear complexes.

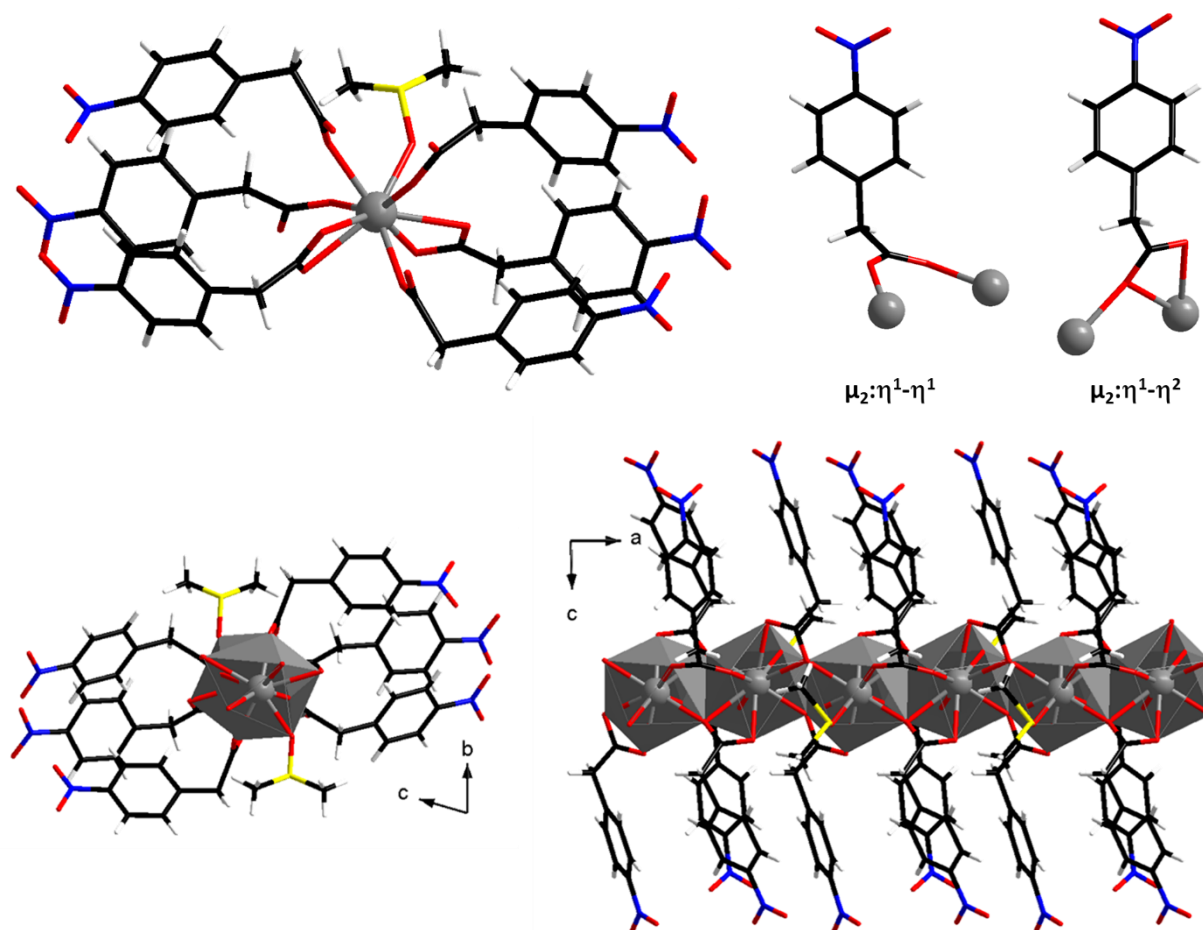


Figure 8. Neighborhood of the Tb^{3+} ion (top left), binding modes of the npa^- ligands (top right) and projection views along the a - and b -axis (bottom left and right, respectively) of $[\text{Tb}(4\text{-npa})]_\infty$.

Because of the length of the ligand the distances between lanthanide ions that belong to neighboring molecular chains are quite long and comprised between 14 Å and 24 Å (Figure 9). The crystal packing is insured by a network of weak hydrogen-bonds and π -stacking interactions between the phenyl groups of adjacent molecular motifs (centroid-to-centroid distances are about 3.8 Å). The DMSO and water crystallization molecules are located in the inter-chains space.

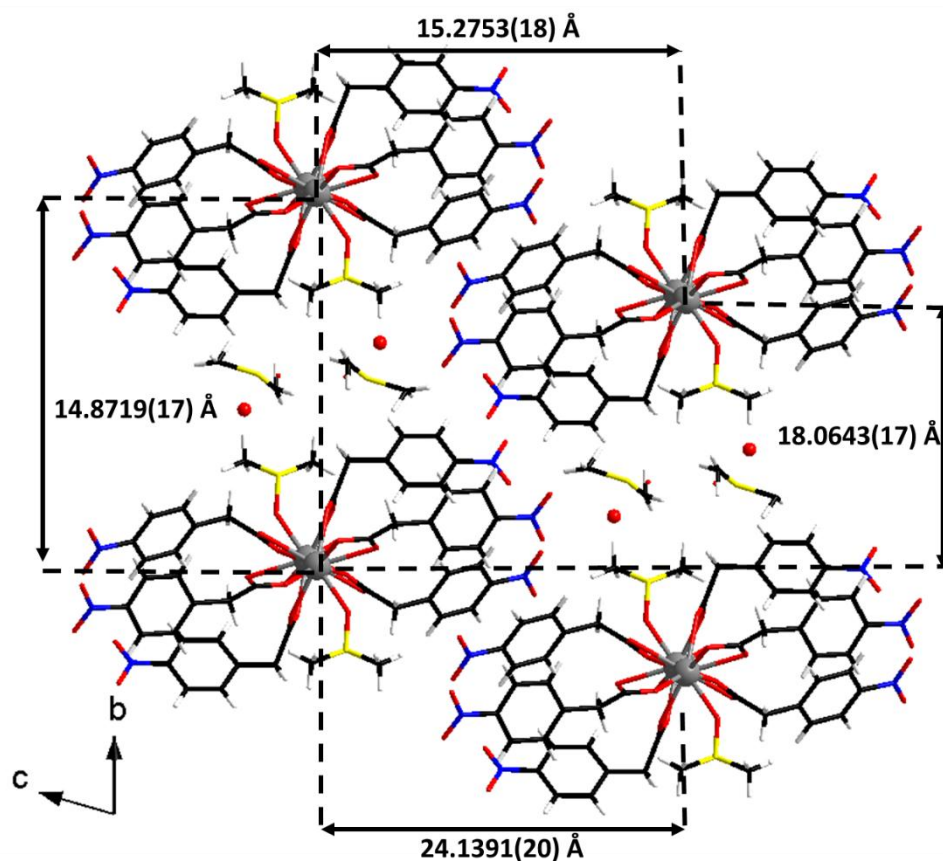


Figure 9. Projection view along the a -axis of four neighboring molecular chains in $[\text{Tb}(\text{4-npa})]_{\infty}$. Shortest distances between Tb^{3+} ions that belong to adjacent molecular chains are indicated.

CONCLUSION AND OUTLOOK.

Five series of pseudo-iso-reticular coordination polymers have been obtained with five different halogeno-benzoate ligands. Additionally, in the same synthetic conditions, another crystal structure has been obtained by replacing halogeno-benzoate ligands by 4-nitro-phenyl-acetate. All the six crystal structures can be described on the basis of original straight chain-like molecular motifs. This strongly supports that the hexa-nuclear complexes used as reactants present a strong structuring effect toward the formation of 1D chain-like coordination polymers. This opens the way to the synthesis of new lanthanide-based coordination polymers that could not be obtained from usual lanthanide salts such as chloride or nitrate. Luminescence studies indicate that, in these compounds, there are strong intermetallic energy transfers that can be modulated by the choice of the halogeno group.

They also strongly suggest that in these systems, the exchange mechanism is important as far as intermetallic energy transfers are concerned. The rationalization of the influence, of the nature of the halogen and that of its position (*meta* or *para*) on the exchange pathways, is out of the scope of this paper but deserves to be studied in the future.

ACKNOWLEDGEMENTS.

The China Scholarship Council Ph.D. Program, a cooperation program with the French UT and INSA, is acknowledged for financial support. The CDIFX (X-ray diffraction center of Rennes) is acknowledged for single-crystals X-ray diffraction data collections.

SUPPORTING INFORMATION.

pH range of the hexa-nuclear entities precipitation *versus* rare-earth ionic radius; Simulated powder X-ray diffraction diagrams; Relative metallic contents; Projection views; Selected intermetallic distances and angles; Shape calculations of the coordination polyhedrons; Halogen-halogen shortest distances; Colorimetric coordinates; Overall quantum yields *vs* x ; Room temperature solid-state emission spectra *versus* x .

REFERENCES.

1. E. W. Berg; A. Alam, Studies on coordination polymers. Part I : Coordination polymers of 8,8'-dihydroxy-5,5'-biquinoyl. *Anal. Chim. Acta* **1962**, 27, 454-459.
2. D. G. Karraker, Coordination of trivalent lanthanide ions. *J. Chem. Educ.* **1970**, 47, 424-430.
3. J. C. G. Bünzli, Benefiting from the unique properties of lanthanide ions. *Accounts Chem. Res.* **2006**, 39, 53-61.
4. R. Sessoli; K. Bernot, Lanthanides in extended molecular networks. In *Molecular magnetism*, Wiley-VCH Verlag GmbH & Co. KGaA: **2015**, p 89-124.
5. R. Sessoli; A. K. Powell, Strategies towards single molecule magnets based on lanthanide ions. *Coord. Chem. Rev.* **2009**, 253, 2328-2341.
6. K. Bernot; C. Daiguebonne; G. Calvez; Y. Suffren; O. Guillou, A Journey in Lanthanide Coordination Chemistry: From Evaporable Dimers to Magnetic Materials and Luminescent Devices. *Accounts Chem. Res.* **2021**, 54, 427-440.
7. J. C. G. Bünzli; S. V. Eliseeva, Intriguing aspect of lanthanide luminescence. *Chem. Sci.* **2013**, 4, 1039-1049.
8. S. V. Eliseeva; J. C. G. Bünzli, Rare earths : jewels for fonctionnal materials of the future. *New J. Chem.* **2011**, 35, 1165-1176.
9. V. Trannoy; A. N. C. Neto; D. S. C. Brites; L. D. Carlos; H. Serier-Brault, Engineering of mixed $\text{Eu}^{3+}/\text{Tb}^{3+}$ Metal-Organic Frameworks luminescent thermometers with tunable sensitivity. *Advanced Optical Materials* **2021**, 2001938.
10. D. S. C. Brites; A. Millan; L. D. Carlos, Lanthanides in Luminescent Thermometry. In *Handbook on the Physics and Chemistry of Rare Earths*, Gschneidner, K. A.; Bünzli, J. C. G.; Pecharsky, V. K., Eds. Elsevier: **2016**; Vol. 49, p 339-427.
11. A. Gamonal; C. Sun; A. L. Mariano; E. Fernandez-Bartolome; E. Guerrero-SanVicente; B. Vlaisavljevich; J. Castells-Gil; C. Marti-Gastaldo; R. Poloni; R. Wannemacher; J. Cabanillas-Gonzalez; J. S. Costa, Divergent adsorption-dependent luminescence of amino-functionalized lanthanide metal-organic frameworks for highly sensitive NO_2 sensors. *J. Phys. Chem. Lett.* **2020**, 11, 3362-3368.
12. J. He, Xu, J. ; J. Yin; N. Li; X.-H. Bu, Recent advances in luminescent metal-organic frameworks for chemical sensors. *Sci China Mater* **2019**, 62, 1655-1678.
13. S. V. Eliseeva; J. C. G. Bünzli, Lanthanide luminescence for fonctionnal materials and bio-sciences. *Chem. Soc. Rev.* **2010**, 39, 189-227.
14. J.-C. G. Bünzli, Lanthanide luminescence for biomedical analyses and imaging. *Chem. Rev.* **2010**, 111, 2729-2755.
15. Y. Cui; J. Zhang; H. He; G. Qian, Photonic functional metal-organic frameworks. *Chem. Soc. Rev.* **2018**, 47, 5740-5785.
16. Y. Cui; J. Zhang; B. Chen; G. Qian, Lanthanide Metal-Organic Frameworks for Luminescent Applications. *Handbook on the Physics and Chemistry of Rare Earths* **2016**, 50, 243-268.
17. Y. Pointel; C. Daiguebonne; Y. Suffren; F. Le Natur; S. Freslon; G. Calvez; K. Bernot; D. Jacob; O. Guillou, Colloidal suspensions of highly luminescent lanthanide-based coordination polymer molecular alloys for ink-jet printing and tagging of technical liquids. *Inorg. Chem. Front.* **2021**, 2125-2135.
18. O. Guillou; C. Daiguebonne; G. Calvez; K. Bernot, A long journey in lanthanide chemistry : from fundamental crystallogenes studies to commercial anti-counterfeiting taggants. *Accounts Chem. Res.* **2016**, 49, 844-856.
19. J. Andres; R. D. Hersch; J. E. Moser; A. S. Chauvin, A new counterfeiting feature relying on invisible luminescent full color images printed with lanthanide-based Inks. *Adv. Func. Mater.* **2014**, 24, 5029-5036.
20. Y.-M. Wang; X.-T. Tian; H. Zhang; Z.-R. Yang; X.-B. Yin, Anticounterfeiting quick response code with emission color of invisible Metal-Organic Frameworks as encoding information. *ACS Appl. Mater. Interfaces* **2018**, 10, 22445-22452.

21. K.-L. Wong; J. C. G. Bünzli; P. A. Tanner, Quantum yield and brightness. *J. Lumin.* **2020**, *224*, 117256.
22. J. C. G. Bünzli, On the design of highly luminescent lanthanide complexes. *Coord. Chem. Rev.* **2015**, *293-294*, 19-47.
23. Y. Pointel; Y. Suffren; C. Daguebonne; F. Le Natur; S. Freslon; G. Calvez; K. Bernot; O. Guillou, Rational design of dual IR and visible highly luminescent light lanthanides based coordination polymers. *Inorg. Chem.* **2020**, *59*, 10673-10687.
24. R. Maouche; S. Belaid; B. Benmerad; S. Bouacida; C. Daguebonne; Y. Suffren; S. freslon; K. Bernot; O. Guillou, Highly luminescent Europium-based heteroleptic coordination polymers with phenantroline and glutarate ligands. *Inorg. Chem.* **2021**, *60*, 3707-3718.
25. T. N. Nguyen; S. V. Eliseeva; C. Y. Chow; J. W. Kampf; S. Petoud; V. Pecoraro, Peculiarities of crystal structures and photophysical properties of GaIII/LnIII metallacrowns with a non-planar [12-MC-4] core. *Inorg. Chem. Front.* **2020**, *7*, 1553-1563.
26. E. V. Salerno; S. V. Eliseeva; B. L. Schneider; J. W. Kampf; S. Petoud; V. Pecoraro, Visible, Near-Infrared, and Dual-Range Luminescence Spanning the 4f Series Sensitized by a Gallium(III)/Lanthanide(III) Metallacrown Structure. *The Journal of Physical Chemistry A* **2020**, *124*, 10550-10564.
27. E. V. Salerno; J. Zeler; S. V. Eliseeva; M. A. Hernandez-Rodriguez; A. N. Carneiro Neto; S. Petoud; V. Pecoraro; L. D. Carlos, [Ga³⁺Sm³⁺, Ga³⁺Tb³⁺] Metallacrowns are Highly Promising Ratiometric Luminescent Molecular Nanothermometers Operating at Physiologically Relevant Temperatures. *Chem. - Eur. J.* **2020**, *26*, 13792-13796.
28. S. V. Eliseeva; E. V. Salerno; B. A. Lopez Berudez; S. Petoud, Dy³⁺ White Light Emission Can Be Finely Controlled by Tuning the First Coordination Sphere of Ga³⁺/Dy³⁺ Metallacrown Complexes. *J. Am. Chem. Soc.* **2020**, *142*, 16173-16176.
29. Y. Cui; B. Li; H. He; W. Zhou; B. Chen; G. Qian, Metal-organic frameworks as platforms for fonctionnal materials. *Accounts Chem. Res.* **2016**, *49*, 483-493.
30. B. Li; H.-M. Wen; Y. Cui; G. Qian; B. Chen, Multifunctional lanthanide coordination polymers. *Prog. Polym. Sci.* **2015**, *48*, 40-84.
31. S. I. Weissman, Intramolecular energy transfer - The fluorescence of complexes of europium. *J. Chem Phys* **1942**, *10*, 214-217.
32. R. G. Pearson, Hard and soft acids and bases - the evolution of a chemical concept. *Coord. Chem. Rev.* **1990**, *100*, 403-425.
33. R. G. Pearson, Hard and soft acids and bases. *J. Am. Chem. Soc.* **1963**, *85*, 3533-3539.
34. M. Fourmigué, Halogen bonding: Recent advances. *Current Opin. Solid St. M.* **2009**, 36-45.
35. J. C. G. Bünzli; S. V. Eliseeva, Basics of lanthanide photophysics. In *Lanthanide Luminescence*, Hänninen, P.; Härmä, H., Eds. Springer Berlin Heidelberg: **2010**; Vol. 7, p 1-45.
36. Y. Pointel; F. Houard; Y. Suffren; C. Daguebonne; F. Le Natur; S. Freslon; G. Calvez; K. Bernot; O. Guillou, High luminance of hetero lanthanide based molecular alloys by phase-induction strategy. *Inorg. Chem.* **2020**, *59*, 11028-11040.
37. A. M. Badiane; S. Freslon; C. Daguebonne; Y. Suffren; K. Bernot; G. Calvez; K. Costuas; M. Camara; O. Guillou, Lanthanide based coordination polymers with a 4,5-dichlorophthalate ligand exhibiting highly tunable luminescence : Toward luminescent bar codes. *Inorg. Chem.* **2018**, *57*, 3399-3410.
38. G. Calvez; F. Le Natur; C. Daguebonne; K. Bernot; Y. Suffren; O. Guillou, Lanthanide-based hexanuclear complexes and their use as molecular precursors. *Coord. Chem. Rev.* **2017**, *340*, 134-153.
39. D. Alezi; A. M. P. Peedikakkal; L. Weselinski; V. Guillermy; Y. Belmabkhout; A. J. Cairns; Z. Chen; L. Wojtas; M. Eddaoudi, Quest for highly connected metal-organic framework platforms : rare earth polynuclear clusters versatility meets net topology needs. *J. Am. Chem. Soc.* **2015**, *137*, 5421-5430.
40. Z. Zheng, Assembling lanthanide hydroxo clusters. *Chemtracts - Inorganic Chemistry* **2003**, *16*, 1-12.

41. L. Huang; L. Han; W. Feng; L. Zheng; Z. Zhang; Y. Xu; Q. Chen; D. Zhu; S. Niu, Two 3D coordination frameworks based on nanosized huge Ln_{26} ($\text{Ln} = \text{Dy}$ and Gd) spherical clusters. *Cryst. Growth Des.* **2010**, *10*, 2548-2552.
42. X.-J. Kong; L.-S. Long; L.-S. Zheng; R. Wang; Z. Zheng, Hydrolytic Synthesis and Structural Characterization of Lanthanide Hydroxide Clusters Supported by Nicotinic Acid. *Inorg. Chem.* **2009**, *48*, 3268-3273.
43. X.-J. Kong; Y. Wu; L.-S. Long; L.-S. Zheng; Z. Zheng, A chiral 60-metal sodalite cage featuring 24 vertex-sharing $[\text{Er}_4(\mu_3\text{-OH})_4]$ cubanes. *J. Am. Chem. Soc.* **2009**, *131*, 6918-6919.
44. Z. Zheng, Cluster compounds of rare-earth elements. In *Handbook on the Physics and Chemistry of Rare Earths*, Gschneidner, K. A.; Bünzli, J. C. G.; Pecharsky, V. K., Eds. Elsevier: **2010**; Vol. 40, p 109-239.
45. G. Giester; Z. Zak; P. Unfried, Syntheses and crystal structures of rare earth basic nitrates hydrates. *J. Alloys Compd.* **2009**, *481*, 116-128.
46. G. Giester; Z. Zak; P. Unfried, Syntheses and crystal structures of rare earth basic nitrates hydrates: Part III. $[\text{Ln}_6(\mu_6\text{-O})(\mu_3\text{-OH})_8(\text{H}_2\text{O})_{12}(\text{NO}_3)_6](\text{NO}_3)_2 \cdot x\text{H}_2\text{O}$, $\text{Ln} = \text{Y}, \text{Sm}, \text{Eu}, \text{Gd}, \text{Tb}, \text{Dy}, \text{Ho}, \text{Er}, \text{Tm}, \text{Yb}, \text{Lu}$; $x=0; 3, 4, 5, 6$. *J. Alloys Compd.* **2009**, *481*, 116-128.
47. G. Giester; P. Unfried; Z. Zak, Syntheses and crystal structures of some new rare earth basic nitrates II : $[\text{Ln}_6\text{O}(\text{OH})_8(\text{H}_2\text{O})_{12}(\text{NO}_3)_6](\text{NO}_3)_2 \cdot x\text{H}_2\text{O}$, $\text{Ln} = \text{Sm}, \text{Dy}, \text{Er}$; $x(\text{Sm})=6$, $x(\text{Dy})=5$, $x(\text{Er})=4$. *J. Alloys Compd.* **1997**, *257*, 175-181.
48. C. L. Lengauer; G. Giester; P. Unfried, $\text{Sm}(\text{OH})_2\text{NO}_3$: synthesis, characterization, powder diffraction data and structure refinement by Rietveld technique. *Powder Diffr.* **1994**, *9*, 115-118.
49. Z. Zak; P. Unfried; G. Giester, The structures of some rare earth basic nitrates $[\text{Ln}_6(\mu_6\text{-O})(\mu_3\text{-OH})_8(\text{H}_2\text{O})_{12}(\text{NO}_3)_6](\text{NO}_3)_2 \cdot x\text{H}_2\text{O}$, $\text{Ln} = \text{Y}, \text{Gd}, \text{Yb}$; $x(\text{Y}, \text{Yb})=4$, $x(\text{Gd})=5$. A novel rare earth metal cluster of the M_6X_8 type with interstitial O atom. *J. Alloys Compd.* **1994**, *205*, 235-242.
50. G. Calvez; C. Daiguebonne; O. Guillou; T. Pott; P. Méléard; F. Le Dret, Lanthanide-based hexanuclear complexes usable as molecular precursor for new hybrid materials : state of the art. *C. R. Chimie* **2010**, *13*, 715-730.
51. P. Unfried; K. Rossmanith, The chemical decomposition of rare earth nitrates : a new method for the enrichment of heavy yttrium earth nitrates in kg-quantities. *Monatsh. Chem.* **1992**, *123*, 1-8.
52. P. Unfried; K. Rossmanith; H. Blaha, Two new basic Yttrium nitrates. *Monatsh. Chem.* **1991**, *122*, 635-644.
53. D. Pelloquin; D. Louër; M. Louër, Powder diffraction studies in the $\text{YONO}_3\text{-Y}_2\text{O}_3$ system. *J. Solid State Chem.* **1994**, *112*, 182-188.
54. G. W. Beal; W. O. Milligan; D. R. Dillin; R. J. Williams; J. J. Mc Coy, Refinement of Neodymium trihydroxide. *Acta Crystallogr. B* **1976**, *32*, 2227-2229.
55. G. Calvez; C. Daiguebonne; O. Guillou, Unprecedented lanthanide containing coordination polymers constructed from hexanuclear molecular building blocks: $\{[\text{Ln}_6\text{O}(\text{OH})_8](\text{NO}_3)_2(\text{bdc})(\text{Hbdc})_2, 2\text{NO}_3, \text{H}_2\text{bdc}\}_n$. *Inorg. Chem.* **2011**, *50*, 2851-2858.
56. F. Le Natur; G. Calvez; C. Daiguebonne; O. Guillou; K. Bernot; J. Ledoux; L. Le Polles; C. Roiland, Coordination polymers based on hexanuclear rare earth complexes : Toward independant luminescence brightness and color emission. *Inorg. Chem.* **2013**, *52*, 6720-6730.
57. O. Guillou; C. Daiguebonne; G. Calvez; F. Le Dret; P. E. Car, Structuring effect of $[\text{Ln}_6\text{O}(\text{OH})_8(\text{NO}_3)_6(\text{H}_2\text{O})_{12}]^{2+}$ entities. *J. Alloys Compd.* **2008**, *451*, 329-333.
58. G. Calvez; K. Bernot; O. Guillou; C. Daiguebonne; A. Caneschi; N. Mahé, Sterically-induced synthesis of 3d-4f one-dimensional compounds: a new route towards 3d-4f Single Chain Magnets. *Inorg. Chim. Acta* **2008**, *361*, 3997-4003.
59. H. Yao; G. Calvez; C. Daiguebonne; K. Bernot; Y. Suffren; O. Guillou, Hetero-hexalanthanide complexes: A new synthetic strategy for molecular thermometric probes. *Inorg. Chem.* **2019**, *58*, 16180-16193.
60. H. Yao; G. Calvez; C. Daiguebonne; K. Bernot; Y. Suffren; M. Puget; C. Lescop; O. Guillou, Hexalanthanide complexes as molecular precursors: synthesis, crystal structure and luminescent and magnetic properties. *Inorg. Chem.* **2017**, *56*, 14632-14642.

61. H. Yao; G. Calvez; C. Daiguebonne; Y. Suffren; K. Bernot; O. Guillou, Hexa-nuclear molecular precursors as tools to design luminescent coordination polymers with lanthanide segregation. **2021**, *60*, 16782-16793.
62. J. F. Desreux, In *Lanthanide Probes in Life, Chemical and Earth Sciences*, Choppin, G. R.; Bünzli, J. C. G., Eds. Elsevier: Amsterdam, **1989**; Vol. Elsevier, p 43.
63. G. Calvez; O. Guillou; C. Daiguebonne; P.-E. Car; V. Guillerme; Y. Gérault; F. L. Dret; N. Mahé, Octahedral hexanuclear complexes involving light lanthanide ions. *Inorg. Chim. Acta* **2008**, *361*, 2349-2356.
64. W. Kraus; G. Nolze, POWDER CELL - A program for the representation and manipulation of crystal structures and calculation of the resulting X-ray powder patterns. *J. Appl. Crystallogr.* **1996**, *29*, 301-303.
65. T. Roisnel; J. Rodriguez-Carjaval, WinPLOTR : a windows tool for powder diffraction pattern analysis. *Materials Science Forum, Proceedings of the Seventh European Powder Diffraction Conference (EPDIC 7)* **2000**, 118-123.
66. G. M. Sheldrick, A short history of SHELX. *Acta Crystallogr. A* **2008**, *64*, 112-122.
67. G. M. Sheldrick; T. R. Schneider, SHELXL : High-Resolution Refinement. *Macromol. Crystallogr. B* **1997**, 319-343.
68. L. J. Farrugia, WinGX suite for smallmolecule single-crystal crystallography. *J. Appl. Crystallogr.* **1999**, *32*, 837-838.
69. L. J. Farrugia, WinGX and ORTEP for Windows: an update. *J. Appl. Crystallogr.* **2012**, *45*, 849-854.
70. P. Sluis; A. L. Spek, BYPASS: an Effective method for the refinement of crystal structures containing disordered solvent regions. *Acta Crystallogr. A* **1990**, *A46*, 194-201.
71. A. S. Chauvin; F. Gumy; D. Imbert; J. C. G. Bünzli, Europium and terbium tris(dipicolinate) as secondary standards for quantum yield determination. *Spectrosc Lett* **2004**, *37*, 512-532.
72. G. Wyszecki, Colorimetry. In *Handbook of Optics*, Driscoll, W. G.; Vaughan, W., Eds. Mac Graw-Hill Book Company: New-York, **1978**, p 1-15.
73. CIE, *International Commission on Illumination - Technical report*. CIE: **1995**; Vol. 13-3, p 16.
74. S. Alvarez; P. Alemany; D. Casanova; J. Cirera; M. Llunell; D. Avnir, Shape maps and polyhedral interconversion paths in transition metal chemistry. *Coord. Chem. Rev.* **2005**, *249*, 1693-1708.
75. C. Piguet; J. C. G. Bünzli; G. Bernardinelli; G. Hopfgartner; A. F. Williams, Self-assembly and photophysical properties of lanthanide dinuclear triple-helical complexes. *J. Am. Chem. Soc.* **1993**, *115*, 8197-8206.
76. W. T. Carnall; P. R. Fields; K. Rajnak, Electronic energy levels of the trivalent lanthanide ions. IV. Eu^{3+} . *J. Chem. Phys.* **1968**, *49*, 4450-4455.
77. W. T. Carnall; P. R. Fields; K. Rajnak, Spectral intensities of the trivalent lanthanides and actinides in solution. II. Pm^{3+} , Sm^{3+} , Eu^{3+} , Gd^{3+} , Tb^{3+} , Dy^{3+} and Ho^{3+} . *J. Chem. Phys.* **1968**, *49*, 4412-4423.
78. L. Prodi; M. Maestri; R. Ziesel; V. Balzani, Luminescent Eu^{3+} , Tb^{3+} and Gd^{3+} complexes of a branched triazacyclononane ligand containing three 2,2'-bipyridine units. *Inorg. Chem.* **1991**, *30*, 3798-3802.
79. S. Quici; M. Cavazzini; G. Marzanni; i. G. Accors; N. Armaroli; B. Ventura; F. Barigelli, Visible and near-infrared luminescence from water soluble Lanthanide complexes. *Inorg. Chem.* **2005**, *44*, 529-537.
80. M. D. Ward, Transition metal sensitized near infrared luminescence from lanthanide in d-f heteronuclear arrays. *Coord. Chem. Rev.* **2007**, *251*, 1663-1677.
81. C. Galaup; J.-M. Couchet; S. Bedel; P. Tisnès; C. Picard, Direct access to terpyridine-containing polyazamacrocycles as photosensitizing ligands for Eu(III) luminescence in aqueous media. *J. Org. Chem.* **2005**, *70*, 2274-2284.
82. S. Freslon; Y. Luo; G. Calvez; C. Daiguebonne; O. Guillou; K. Bernot; V. Michel; X. Fan, Influence of photo-induced electron transfer on lanthanide-based coordination polymers

luminescence : A comparison between two pseudo-isorecticular molecular networks. *Inorg. Chem.* **2014**, *53*, 1217-1228.

83. W. T. Carnall; P. R. Fields; K. Rajnak, Energy levels in the trivalent lanthanide ions. III. Tb³⁺. *J. Chem. Phys.* **1968**, *49*, 4447-4450.

84. D. T. Clark; J. N. Murrell; J. M. Tedder, The magnitudes and signs of the inductive and mesomeric effects of the halogens. *Journal of the Chemical Society* **1963**, 1250-1253.

85. D. L. Dexter, A theory of sensitized luminescence in solids. *J. Chem. Phys.* **1953**, *21*, 836-850.

86. T. Förster, *Comparative effects of radiation*. John Wiley & Sons: New-York, **1960**.

87. P. Dechambenoit; S. Ferlay; N. Kyritsakas; M. W. Hosseini, Playing with isostructurality : from tectons to molecular alloys and composite crystals. *Chem. Comm.* **2009**, 1559-1561.

88. N. Kerbellec; D. Kustaryono; V. Haquin; M. Etienne; C. Daiguebonne; O. Guillou, An Unprecedented Family of Lanthanide-Containing Coordination Polymers with Highly Tunable Emission Properties. *Inorg. Chem.* **2009**, *48*, 2837-2843.

89. V. Haquin; M. Etienne; C. Daiguebonne; S. Freslon; G. Calvez; K. Bernot; L. Le Polles; S. E. Ashbrook; M. R. Mitchell; J. C. G. Bünzli; O. Guillou, Color and brightness tuning in hetero-nuclear lanthanide teraphthalate coordination polymers. *Eur. J. Inorg. Chem.* **2013**, 3464-3476.

90. X. Fan; S. Freslon; C. Daiguebonne; L. Le Polles; G. Calvez; K. Bernot; O. Guillou, A family of lanthanide based coordination polymers with boronic acid as ligand. *Inorg. Chem.* **2015**, *54*, 5534-5546.

91. A. Abdallah; S. Freslon; X. Fan; A. Rojo; C. Daiguebonne; Y. Suffren; K. Bernot; G. Calvez; T. Roisnel; O. Guillou, Lanthanide based coordination polymers with 1,4 carboxyphenylboronic ligand: multi emissive compounds for multi sensitive luminescent thermometric probes. *Inorg. Chem.* **2019**, *58*, 462-475.

92. I. Badiane; S. Freslon; Y. Suffren; C. Daiguebonne; G. Calvez; K. Bernot; M. Camara; O. Guillou, High britness and easy color modulation in lanthanide-based coordination polymers with 5-methoxyisophthalate as ligand: Toward emission colors additive strategy. *Cryst. Growth Des.* **2017**, *17*, 1224-1234.

93. F. Auzel, Upconversion and Anti-Stokes Processes with f and d Ions in Solids. *Chem. Rev.* **2004**, *104*, 139-173.

94. F. Auzel, History of upconversion discovery and its evolution. *J. Lumin.* **2020**, *223*, 116900.

95. L. Aboshyan-Sorgho; M. Cantuel; S. Petoud; A. Hauser; C. Piguet, Optical sensitization and upconversion in discrete polynuclear chromium–lanthanide complexes. *Coord. Chem. Rev.* **2012**, *256*, 1644-1663.

96. M. Inokuti; F. Hirayama, Influence of Energy Transfer by the Exchange Mechanism on Donor Luminescence. *J. Chem. Phys.* **1965**, *43*, 1978-1989.

97. V. I. Tsaryuk; K. P. Zhuravlev; V. F. Zolin; V. A. Khudryashova; J. Legendziewicz; R. Szostak, Luminescence efficiency of aromatic carboxylate pf europium and terbium when methylene bridges and nitro groups are present in the ligand. *Journal of Applied Spectroscopy* **2007**, *74*, 51-59.

98. H. C. Brown, *Determination of Organic Structures by Physical Methods V4* Academic Press Inc.: New-York, **1971**.

99. D. Casanova; M. Llunell; P. Alemany; S. Alvarez, The rich stereochemistry of eight-vertex polyhedra: A continuous shape measures study. *Chem. - Eur. J.* **2005**, *11*, 1479-1494.

TABLE OF CONTENT

Six series of coordination polymers are prepared from octahedral hexa-nuclear molecular precursors. All of them can be described on the basis of original straight chain-like molecular motifs.

